2006-03-26

Gas Chromatography: Mass Spectrometry of Chemical Agents and Related Interferents

Lailiang Zhai
Brigham Young University - Provo

GAS CHROMATOGRAPHY-MASS SPECTROMETRY OF CHEMICAL AGENTS AND RELATED INTERFERENTS

by

Lailiang Zhai

A thesis submitted to the faculty of

Brigham Young University

in partial fulfillment of the requirements for the degree of

Master of Science

Department of Chemistry and Biochemistry

Brigham Young University

April 2006

BRIGHAM YOUNG UNIVERSITY

GRADUATE COMMITTEE APPROVAL

of a thesis submitted by

Lailiang Zhai

This thesis has been read by each member of the following graduate committee and by majority vote has been found to be satisfactory.

_____	_____
Date	Milton L. Lee, Chair
_____	_____
Date	Matthew R. Linford
_____	_____
Date	David V. Dearden
_____	_____
Date	Delbert J. Eatough

BRIGHAM YOUNG UNIVERSITY

As chair of the candidate's graduate committee, I have read the thesis of Lailiang Zhai in its final form and have found that (1) its format, citations and bibliographical style are consistent and acceptable and fulfill university and department style requirements; (2) its illustrative materials including figures, tables, and charts are in place; and (3) the final manuscript is satisfactory to the graduate committee and is ready for submission to the university library.

_____	_____
Date	Milton L. Lee Chair, Graduate Committee
_____	_____
Date	David V. Dearden Graduate Coordinator
_____	_____
Date	Thomas W. Sederberg Associate Dean, College of Physical and Mathematical Sciences

ABSTRACT

GAS CHROMATOGRAPHY-GAS CHROMATOGRAPHY OF CHEMICAL AGENTS AND RELATED INTERFERENTS

Lailiang Zhai

Department of Chemistry and Biochemistry

Master of Science

One of the main problems encountered in chemical analysis operations in the field is collecting sufficient sample from the source and transferring that sample to the measurement instrument for fast separation and identification. I have been involved in developing a field-portable gas chromatography-mass spectrometry (GC-MS) system with solid phase microextraction (SPME) sampling for point detection of chemical agents. The objective is to minimize the analysis time between sampling and detection of a potential chemical threat. SPME offers a convenient means for sampling gaseous and liquid samples, concentrating the analytes, and transferring the analytes to the injection port of a GC system for separation and identification. GC-MS has advantages of high efficiency, speed, and applicability for field analysis.

Work was done to optimize the SPME fiber coating, capillary column dimensions, and GC operating conditions to provide complete analysis within 3 minutes. Since isothermal operation of the GC was a prior requirement, many components in the chromatograms were unresolved. Therefore, a peak de-convolution algorithm was applied to allow for identification and quantitation of poorly resolved and often completely obscured trace components. Details of the instrumentation and optimization of operating conditions are described in this thesis.

ACKNOWLEDGEMENTS

I would like to express my gratitude to many people. The completion of this thesis and the research work would not have been possible without their support.

First of all, I want to express heartfelt gratitude to my advisor, Dr. Milton L. Lee, for giving me the opportunity to study under his supervision. I thank him for his guidance, encouragement, support and friendship throughout my graduate work. I have learned from him not only how to be successful in my career, to be a good scientist, but also how to be a respectable person in my personal life.

I thank all of my committee members, Dr. David V. Dearden, Dr. Matthew R. Linford, and Dr. Delbert J. Eatough, for their encouragement and valuable suggestions.

I thank Dr. Edgar D. Lee, Dr. H. Dennis Tolley, James R. Oliphant, Randall W. Waite and Jeffrey L. Jones for their helpful suggestions and insightful advice on experimental design and instrumentation.

I would like to thank Susan L. Tachka, in particular, for her help in learning English and her daily encouragement during my stay. I really experienced a feeling of family life here because of her hard work. I also thank the students in Dr. Milton L. Lee's group and in the department who have worked with me and helped me during my stay.

Special thanks are expressed to my parents, brother and sister. It would not have been possible for me to achieve my educational goal without their giving me the opportunity, encouragement, and long-lasting support.

Finally, I would like to thank the Department of Chemistry and Biochemistry as well as Brigham Young University for providing financial support and an opportunity to study here.

TABLE OF CONTENTS

LIST OF TABLES

LIST OF FIGURES

Chapter 1. Introduction

1.1 Purpose

The purpose of this work was to develop and optimize a gas chromatographic (GC) method that could be used in the field to identify chemical agents. In my studies, I examined two aspects of the proposed method: (a) field sampling using solid phase microextraction (SPME) and (b) column and operating conditions for GC analysis.

Chemical warfare agents were first used in large amounts during World War I, and have been used several times in conflicts throughout the world. Because of their potential for mass destruction, prohibition of the development, production, stockpiling and use of chemical weapons was formalized in the 1997 Chemical Weapons Convention.[1] These toxic chemicals and their precursors that have been identified for the application of verification measures are listed in Schedules 1-3 in the Annex on Chemicals of the Chemical Weapons Convention. Analysis of chemical warfare agents and related compounds is an important problem in current research.[2-5] Developing an analytical method capable of detecting and identifying chemical warfare components and their precursors or degradation products has become the focus of many research groups.

Gas chromatography-mass spectrometry (GC-MS) can be used to identify unknown compounds based on their retention parameters, and interpretation of mass spectral fragmentation patterns. The combination of GC and MS is capable of detecting a wide range of toxic agents, providing high selectivity and sensitivity, as well as providing structural information about these compounds.[2-3, 6] Although a number of detectors are being used in confirming the existence of chemical agents, it is generally agreed that

confirmation of the presence of chemical warfare agents and their degradation products requires identification by MS. [7]

1.2 Detection Portability

Field portable GC-MS is desirable for organic compound detection and identification. To date such instruments have suffered from low sensitivity and low resolution compared to their traditional counterparts. Nevertheless a need exists for a portable GC-MS system. This is because of the need for immediate answers in certain applications and also because in-laboratory confirmation runs the risk of losing volatile compounds during transportation. Field portable GC-MS systems have been successfully used in four major application categories:[8] environmental, diagnostics, forensics, and emergency response.

When the technology was first used, field-portable referred to transportable, man-portable, and even better, hand-portable. Meuzelaar et al.[9] defined field-portability as the ability to: (a) perform in-situ, rather than on-site, analysis, (b) obtain information about transient events on a near real-time basis, (c) map out complex gradients and (d) accurately locate point sources.

There are several different types of detection methods that have been used as rapid screening techniques in the field. These include colorimetric, infrared, surface acoustic wave (SAW) sensors, and ion mobility spectrometry (IMS). However, these methods are effective only when used for analyzing specific classes of chemicals, particularly those having low background interferents. On the other hand, GC-MS can provide detailed information about specific compounds with high sensitivity; these advantages make field-portable GC-MS more widely used than other methods.

During the GC-MS analysis process, a mixture usually is sampled, injected into the GC (sample introduction zone), separated into its components (separation zone), and detected (detection zone) using the MS. Finally the data are processed and analyzed (data analyzing zone). Each zone is separate, yet interrelated. The miniaturization of GC-MS involves primarily the GC oven and MS analyzer.

Researchers have used a variety of methods to design and construct field-portable GC-MS systems. The first portable GC-MS prototype was developed at Lawrence Livermore National Laboratory.[10] This system weighed 35 kg and was used to analyze hazardous substances. The laboratory is currently developing a newer version of this portable GC-MS system[11] based on a commercially available portable GC (Model 8610, SRI instruments, Torrance, CA, USA) and compact double-focusing MS,[12-13] allowing separation of three samples within 30 s using a 30 m long column, 2 s scan rate, resolving power of 125, and 10-150 Da mass range.

A GC-MS designed to be contained in a suitcase for field portable organic chemical analysis was invented in 1996.[14] This instrument weighed 27.3 kg, required a peak power consumption of less than 300 watts, had a mass range of 10-650 amu, a resolving power of no less than 1000, used hydrogen as carrier gas, and could be programmed to function up to 280 ˚C.

Shortt et al.[15] integrated a micro GC[16] and a Paul quadrupole ITMS.[17-18] This equipment weighed only 5.4 kg (including turbomolecular and backing pumps), and required only 42 W of power. Although the mass range was narrow, all other aspects, such as mass resolution, sensitivity, etc., were all comparable to its commercial

counterpart.[15] Other systems include Hewlett Packard MSD based GC-MS systems[19-20] and a hand-portable prototype.[21]

There are several new approaches to portable GC-MS systems. Low thermal mass GC-MS is a novel approach that is well suited for field GC-MS.[72] This technique was first described by Hail et al.[23] Several configurations are currently available,[22,24-28]and their performances were evaluated by Sloan et al.[27] Another approach is called transfer line GC (TLGC), in which a short, narrow-bore column is used as an interface between the MS and a sampling system, typically for a process that must be analyzed on line.[29] The column acts both as the flow restrictor for the MS pumping system and as the separation column for the sample. Several studies were conducted by Doherty et al.[30-32] and the theory for this method was provided by Arnold et al.[33]

1.3 GC Separation and Detection

Fundamentally, a GC-MS involves two steps for analyzing and identifying a sample. GC is a technique based on the partition (or adsorption) of analytes between a gaseous mobile phase and a liquid (or solid) phase immobilized on the surface of an inert solid in a small diameter tube (the column). A GC is an apparatus that is used to separate a mixture into its different components according to the interaction of the components with the liquid (or solid) stationary phase. After the components are separated, they arrive at the output of the GC where they are identified.

A conventional GC requires a bulky oven, which is power inefficient, heavy to carry, and has relatively slow temperature programming rates, usually allowing at most 75˚C/min. Miniaturizing GC usually involves miniaturizing the column oven, which has the largest thermal mass in a GC system. There are four possible ways of reducing the

mass of the traditional oven and thus increasing its maximum heating rate:[34] (a) build a smaller traditional oven[35] or reduce the volume of a traditional oven by adding insulating material; (b) wrap a capillary column around a heated metal cylinder, thus allowing the components to take up a smaller volume; (c) micro-machine a capillary column into a small silicon wafer; and (d) sheath the capillary column with an electrically conducting material.[36-37]

Yost et al.[23] designed a compact GC probe for use in GC-MS. Aluminum-clad columns coiled around a 2.5 in. diameter Teflon spool were covered with Nextel glass braid insulation. Copper connector slides were used to electrically connect the ends of the columns, allowing them to be heated resistively. Because of the very low thermal mass of a column, it could be heated at a rate of 524 ˚C/min (with an initial rate of 2400 ˚C/min) from 50 ˚C to 150 ˚C and cooled down at a rate of 165 ˚C/min (also with a initial rate of 2400˚C/min) from 150˚C to 50 ˚C. The maximum heating rate for a traditional GC oven from 50 ˚C to 150 ˚C is approximately 50 ˚C/min[38], with an approximate cool-down time of 4 min for the same temperature range, or about 7 times longer. The total power required to resistively heat the 2.3 m column to 150 ˚C was approximately 35 W,[23] whereas 2400 W is needed for a conventional oven under exactly the same conditions.[38] Resistively heated columns are extremely attractive for use in miniaturizing GC instrumentation.

Another attractive method being used in the miniaturization of GC is microfabrication. Starting in the 1970's at Stanford,[39] investigators began working to produce a micro-GC on a silicon wafer. More recently, Sacks[40] produced a 3 m long microfabricated column that occupies 3.2 cm x 3.2 cm. Sixteen gaseous components

were separated within 75 s using this column, and approximately 4900 theoretical plates were achieved. Sacks[41] believes that the theoretical plate value is below the actual plate number because the current theories to predict plate number are difficult to use for channel geometries that are not round. Microfabrication typically produces channels that are not round, which are difficult to coat homogeneously.

GC is used to resolve mixtures of compounds into less complex mixtures or into pure components, or it is used for sample preparation and/or clean up prior to final analysis. It can also provide retention data to be used as complementary information for positive identification of resolved components. It is generally accepted that high correlation of retention data between an unknown and a selected reference compound on two columns of different polarity is sufficient for the positive identification of an unknown.[42]

Kováts retention indices have been used in tabulating chromatographic retention data. The advantage of using Kováts indices instead of relative retention times, capacity ratios, or retention volumes is that Kováts indices are independent of the column dimensions, stationary phase, phase ratio, or coating film thickness.

Many measuring techniques are used to monitor analytes eluting from a GC. A flame ionization detector (FID) utilizes a hydrogen-oxygen flame that contains very few ions, and the ionization current increases when the particles of the eluting substances collide with high-energy particles. Thermal conductivity detection (TCD) is based on changes in the electrical conductivity of materials. Other types of detectors, such as the photoionization detector (PID), flame photometric detector (FPD), etc., are also widely

used as detectors for GC. Yet, very limited structural information was available from GC detectors until Gohlke[43] directed the GC effluent into an MS.

MS is the art of "weighing" individual atoms and molecules to determine their masses or molecular weights.[44] MS also provides information about: (a) the elemental composition of samples of matter; (b) the structures of inorganic, organic, and biological molecules; (c) the qualitative and quantitative composition of complex mixtures; (d) the structure and composition of solid surfaces; and (e) the isotopic ratios of atoms in samples.[45] In GC-MS, sample molecules are typically ionized either by an ionizing agent in chemical ionization MS (CIMS), or a beam of high-energy electrons in electron ionization MS (EIMS); the ions undergo specific fragmentation, i.e., bonds break and new bonds form, from which the structure of the molecule can be interpreted.

GC-MS provides considerable information about many types of analytes, including volatile and semi-volatile organic compounds, and has resulted in a technique of considerable importance in the field of chemical analysis. During the past several decades, field-portable GC-MS has gained much attention.

1.4 Feasibility (GC Discrimination)

The overall objective of the project was to separate and identify 25 chemical warfare agents from 25 simulants and interferents. Since chemical warfare agents cannot be tested at the university, a list of their simulants and interferents was chosen for study. From the literature, it is clear that most of the compounds are hard to separate from each other, especially in a single analysis.[46] Figure 1.1 shows the overlap of retention indices and relative elution of some of the chemical warfare agents, simulants, and interferents. Figure 1.1 was drawn based on the assumption that there is certain variation in the

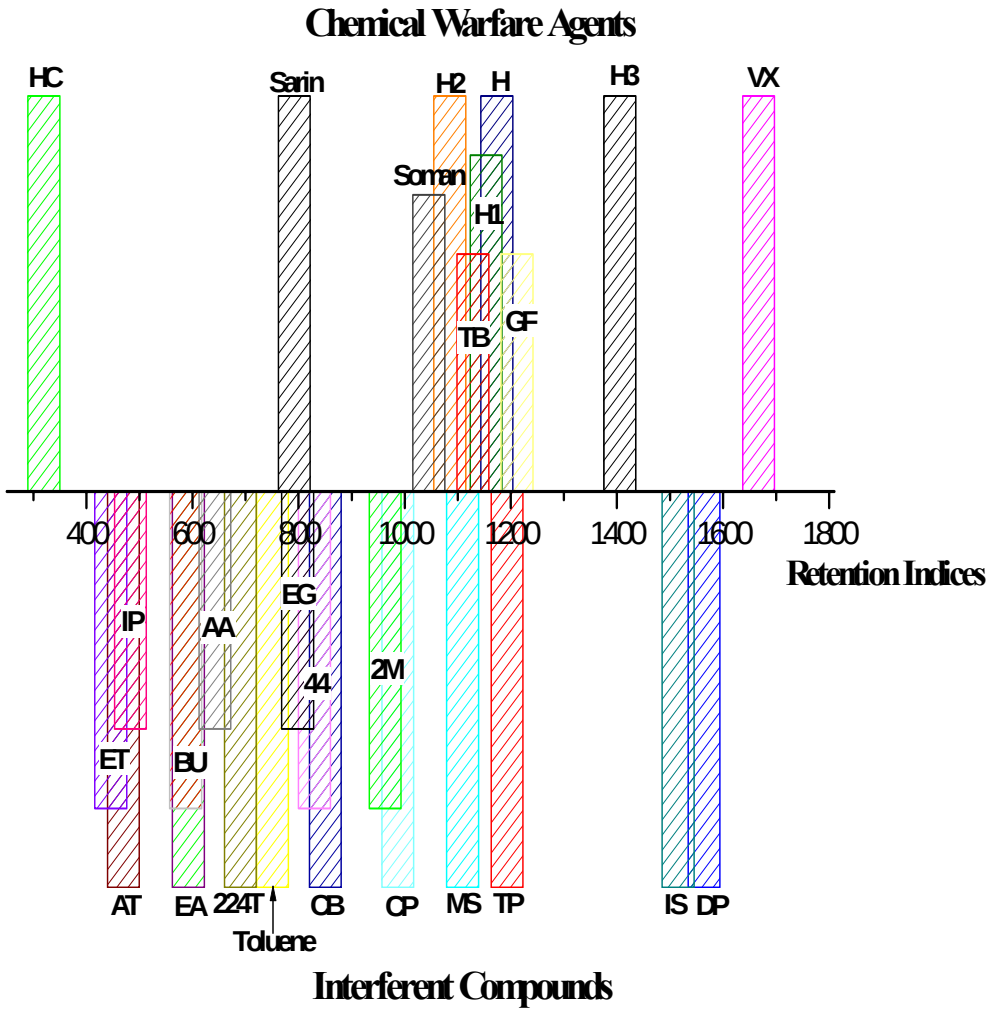

Figure 1.1 Retention indices of some chemical warfare agents, simulants and interferents. Refer to Appendix B for abbreviations.

retention indices. The variation was estimated to be within $\pm$ 30 index units of any specific retention index. It is easy to see that the figure is crowded in certain areas; some of the retention indices are so close to each other that it is very hard to separate them. Although the ultimate goal was to identify all of these compounds under isothermal conditions, PTGC was also used in order to obtain some idea of the temperature effects on these chemicals. Table 1.1 gives a list of the simulants and interferents that were studied.

1.5 Plan

The objective of this thesis was to develop and optimize a method that could be applied for field-portable GC-MS analysis of chemical agents. This thesis reports the rationale and experiments conducted to select the GC column and investigation of the column elution temperature profile for separation of chemical agents, simulants and interferents. SPME fiber selection and optimization of SPME conditions are also included in this thesis.

Table 1.1 Properties and sources of chemical agent simulants and interferents.

Name	Source	Grade	F. W.	M.P. (˚C)	B.P. (˚C)
Isopropanol	Fisher	Reagent	60.1	-88.5	82.4
Ethyl acetate	Mallinckrodt	AR	88.1	-83.6	77.1
Isobutyl alcohol	Fisher	Reagent	74.1	-108	107.9
Ethylene glycol	Fisher	Reagent	62.1	-13	195
Pinacolyl alcohol	Aldrich	98	102.2	4.8	120
Toluene	Fisher	HPLC	92.1	-93	110.6
Dimethyl formamide	Fisher	Reagent	73.1	-61	153
Dimethyl sulfoxide	Mallinckrodt	SpectrAR	78.1	18.45	189
4-Hydroxy-4-methyl-2-pentanone	Aldrich	99%	116.2	-42.8	166
Chlorobenzene	Mallinckrodt	AR	112.6	-45.6	130
DMMP	Aldrich	97%	124.1	-50	181
2-Methyl-2,4-pentanediol	EM Science	99%	118.2	-40	198
2-Chlorophenol	ACROS Organics	98+%	128.6	7	175.6
1-Methyl-2-pyrrolidone	Riedel deHaen (Aldrich)	99.5+%	99.1	-24	202
Diethyl malonate			160.1	-50	199
Triethyl phosphate	Sigma	99.8+%	182.2	-56.4	215
2,2-Thiodiethanol	Fluka	99+%	122.2	-15~-12	165
Methyl salicylate	Fisher	Reagent	152.1	19.4	220~224
Chloroacetophenone	Aldrich	98%	154.6	54-59	244-245
Isoamyl salicylate	Aldrich	98+%	208.3	-75	227-228
Chlorobenzylidene malononitrile	Aldrich	96%	188.6	94~96	310-315
Diethyl phthalate			222.2	-3	298
Tributyl phosphate	Aldrich	99+%	266.3	-80	289
Parathion	Supelco	Neat	291.3	6.1	375

Chapter 2. Solid Phase Microextraction

2.1 Background

Solid phase microextraction or SPME was developed by Belardi and Pawliszyn in 1989 as a method of taking a sample from a liquid and injecting it into a GC system. SMPE fibers became commercially available in 1993 through the introduction of 100 μm i.d. polydimethylsiloxane (PDMS) coated fibers. Since then, many additional fiber coatings, such as polyacrylate, polydimethylsiloxane/divinylbenzene (PDMS/DVB), carbowax/divinylbenzene (CW/DVB), etc., have been manufactured and are also commercially available. SPME has been extensively studied for the analysis of volatile compounds, semi-volatile organic compounds, and especially for environmental matrices. Several handling devices have even been developed and patented. Extraction of specific analytes using different fiber materials has been compared; however, only one review article[47] and two books[48-49] have been published regarding the topic.

SPME is a simple and versatile sampling technique. It was introduced as a modern alternative to complicated and laborious sample preparation technology. Traditionally, the goal of sample preparation has been to introduce samples into analytical equipment in a manner that maximizes the concentration of the analyte of interest and minimizes the concentration of interferents. This increases the detector sensitivity for the analytes and lowers the detection limits. Traditional methods, such as solid phase extraction, liquid-liquid extraction and Soxhlet extraction, remove analytes from the original sample into a different phase. However, SPME does not work this way. SPME employs a fiber coated with solid, liquid or both. The fiber coating adsorbs (for solid coatings) or absorbs (for liquid coatings) analytes from the original sample, the

amount of sample transferred to the fiber coating being proportional to the concentration of the compound in the sample. Quantitation can be achieved through careful control of the parameters used for sampling. The advantage of SPME is that it has the ability to extract a broad range of organic compounds (volatile and semi-volatile) from aqueous samples. SPME is fast, inexpensive, solvent-free, and easy to automate[50] when compared to other extraction methods. SPME combines sampling and pre-concentration steps and allows direct introduction of the analytes into the GC system through a standard split/splitless injection port.[51]

In SPME, a short solid rod of fused silica coated with absorbent polymer is typically used. Equilibrium is established between the concentrations of the analyte in the sample and in the polymer coating for the direct extraction mode, or among the concentrations of the analyte in the sample solution, the gas phase above the sample, and the polymer coating for headspace sampling. Extraction is usually performed in a sealed vial containing the sample. The fiber is immersed directly in the aqueous solution or exposed to the headspace of the vial. A desorption step is needed following sampling.

SPME has been used in a variety of research areas, including environmental,[52-53] pharmaceutical,[54-57] biological[58-60] and food,[61] as well as for chemical warfare agents; SPME-GC-nitrogen-phosphorus detection[62] was used to detect sarin, soman, tabun, and VX in aqueous solution, and SPME was also used to extract a variety of chemicals controlled by the Chemical Weapons Convention from environmental samples during field analysis.[63] An analytical procedure involving in-situ derivatization of degradation products of chemical warfare agents was developed using SPME-GC/MS.[64] Sarin was collected by SPME and analyzed both in the laboratory[65] and on-site.[66] A passive SPME

field sampling method[67] was used to detect airborne hydrogen cyanide, and headspace SPME was used for sampling sulfur mustard in soil.[68] Different commercially available SPME fibers were compared, and PDMS was used in analyzing O-ethyl-S-(2-diisopropylaminoethyl) methylphosphonothiolate,[69] although it was found that a 65 μm PDMS/DVB fiber was the best choice for extraction of nerve agents.[62]

Chemical warfare agent simulants have structures and properties that mimic the real agents; in most cases, simulants were used to imitate a chemical agent without the negative effects. Unfortunately, chemical agent detection and monitoring equipment can respond to the presence of substances other than those for which they are designed to identify. The substances that cause false alarms are known as interferents. Since chemical warfare agent simulants and interferents can give false-positive and false-negative results, all of these compounds require study in order to differentiate them from their more harmful chemical warfare agent counterparts.

In this chapter, twenty-four simulant and interferent compounds were analyzed in order to choose the best fiber for field use. All of the fibers that are commercially available were evaluated. Factors that affect field use were studied statistically via design of experiments.

2.2 Formulas

The amount of sample absorbed into the fiber coating for direct liquid sampling can be expressed as[70]

$$n_f = \frac{\kappa_{fs} V_f V_s C_o}{\kappa_{fs} V_f + V_s} \tag{2.1}$$

and for headspace sampling can be expressed as[71]

$$n_f = \frac{\kappa_{fs} V_f V_s C_o}{\kappa_{fs} V_f + \kappa_{hs} V_h + V_s} \quad (2.2)$$

where n_f is the amount of analyte extracted by the fiber coating, C_o is the initial aqueous concentration of analyte in the sample, κ_{fs} is the distribution constant of the analyte between coating and aqueous phase, κ_{hs} is the partition coefficient of the analyte between coating and headspace phase, V_s is the volume of the aqueous solution, V_f is the volume of the polymer coating, and V_h is the volume of gas phase in the vial.

From equations (2.1) and (2.2), we can infer that SPME sensitivity can be improved through several parameters, such as fiber coating thickness (V_f), coating/aqueous distribution constant (κ_{fs}) of the analyte, etc. Selectivity can also be altered by modifying the chemical structure of the polymer or changing the coating thickness.

2.3 Experimental Conditions

2.3.1 Variables

The variables considered in this work that affect the detection of the target analytes included: user, fiber (two were randomly selected), sample concentration, sampling time, desorption time, and sampling method. Many factors affected the selection of the best fiber. According to the rule "like dissolves like," a fiber with a polar coating should be used for polar analytes. A non-polar coating will absorb non-polar compounds, while polar coatings will have a stronger affinity for polar compounds. Properties of the target analytes should be taken into consideration, such as polarity, functionality, shape, molecular weight, vapor pressure and boiling point. The detection limits and linear range should also be considered, especially for quantitative analysis.

Additional attention must be paid to the mechanism of fiber extraction. Sampling with SPME fibers is based on two mechanisms: adsorption and absorption. Absorption type fibers involve partitioning to extract analytes while adsorption type fibers rely on surface interactions to bind the analytes. Usually, adsorbent fibers have limited capacity, and analytes may compete with each other for adsorption sites. Table 2.1 lists the polarity and extraction mechanism for each of the commercially available fibers.

2.3.2 Experimental Design

When one needs to screen a large number of parameters to identify which ones are important, a design that allows for testing the largest number of factors with the least number of experiments is needed. One popular screening design is the Planckett-Burman design. The purpose of such a screening design is to reduce the number of factors that should be considered. This is done by focusing the initial analysis on the main effects only. Plackett-Burman designs were first reported in 1946, and the theory and application of the experimental design was reviewed by Brereton and Davies.[72-73] Plackett-Burman designs are useful in screening experiments in which many factors are analyzed. They allow us to examine which factors are significant and whether the interactions of two variables are significant. Interactions between more than two variables are assumed to be zero. In the Plackett-Burman design used here, 12 experiments were constructed to investigate six parameters that would most likely influence detection of a test mixture (see Table 2.2).

2.4 Experimental

2.4.1 Chemicals and Materials

All standard chemicals used in this work are listed in Table 1.1 and were used

Table 2.1 Properties of commercially available SPME fibers and their extraction mechanisms (based on Supelco literature T400156).

SPME fiber type	Extraction mechanism	Polarity
PDMS	Absorption	Nonpolar
Polyacrylate (PA)	Absorption	Polar
Carboxen/PDMS	Adsorption	Bipolar
CW/DVB	Adsorption	Polar
DVB/Carboxen/PDMS	Adsorption	Bipolar
PDMS/DVB	Adsorption	Bipolar

Table 2.2 Plackett-Burman design matrix.

Design #	Pattern	User	Fiber[a]	Sample	Exposure[b] (min)	Sampling	Desorp[c] (min)
1	+ + + + + +	A	CAR/PDMS	Conc.	2	Static	1
2	– + – + + +	B	CAR/PDMS	Diluted	2	Static	1
3	– – + – + +	B	CW/DVB	Conc.	8	Static	1
4	+ – – + – +	A	CW/DVB	Diluted	2	Stirred	1
5	– + – – + –	B	CAR/PDMS	Diluted	8	Static	5
6	– – + – – +	B	CW/DVB	Conc.	8	Stirred	1
7	– – – + – –	B	CW/DVB	Diluted	2	Stirred	5
8	+ – – – + –	A	CW/DVB	Diluted	8	Static	5
9	+ + – – – +	A	CAR/PDMS	Diluted	8	Stirred	1
10	+ + + – – –	A	CAR/PDMS	Conc.	8	Stirred	5
11	– + + + – –	B	CAR/PDMS	Conc	2	Stirred	5
12	+ – + + + –	A	CW/DVB	Conc.	2	Static	5

[a]CAR/PDMS = carboxen/polydimethylsiloxane
[a]CW/DVB = carbowax/divinylbenzene
[b]Exposure time = time fiber immersed in sample (min)
[c]Desorp = desorption time (min)

without further purification. The fibers (Supelco, Bellefonte, PA) evaluated included polydimethylsiloxane (PDMS, 100 μm, 30 μm and 7 μm film thicknesses), polydimethylsiloxane/divinylbenzene (PDMS/DVB, 65 μm film thickness), polyacrylate (85 μm film thickness), carboxen™ /polydimethylsiloxane (CAR/PDMS, 75 and 85 μm film thickness), carbowax®/divinylbenzene (CW/DVB, 65 and 70 μm film thickness), and divinylbenzene/ carboxen/polydimethylsiloxane (DVB/CAR/PDMS, 50/30 μm and 50/30 μm film thicknesses). Prior to use, all fibers were conditioned as suggested by the manufacturer.

2.4.2 Instrumentation

Analyses were carried out using an Agilent 6890 series GC coupled with a 5973 mass selective detector (MSD) (Agilent Technologies, Wilmington, DE). Separations were accomplished using a 10 m × 0.1 mm i.d., 0.2 μm film thickness DB-5 column (Agilent Technologies). Helium was used as the carrier gas with a linear velocity of 34 cm/s. The injector was maintained constant at 250 ˚C and the oven temperature was held at 130 ˚C. The SPME fibers after sampling were desorbed for 2 min using the splitless mode (split activated after 2 min). The temperature of the transfer line between the GC and the MSD was maintained at 250 ˚C and the ion source was at 230 ˚C. Mass spectra were scanned over the range of 35-350 m/z.

The selection of the best fiber from the commercially available fibers was accomplished using temperature programmed GC. The original sample was diluted 100 times with water to reach an analyte concentration in the ppm range. For each run, a 2 mL volume of the test solution was transferred to a 4 mL vial. The sampling end of the fiber was immersed in the sample for 5 min. The fiber was then retracted into the

protective sheath and inserted into the GC injection port. The fiber was positioned in the middle of the liner (0.75 mm i.d., Bellefonte, PA) for desorption. All of the separations were carried out under temperature programmed GC conditions. The oven temperature was set at 35 ˚C for 1 min and then increased to 200 ˚C at a rate of 4˚C/min. The solution in the vial was discarded after each extraction, and a fresh solution was used to test each new fiber in order to keep all of the conditions in the experiments the same. The fiber that gave the best sensitivity and absorbed the most compounds was used for optimizing the operating conditions.

2.5 Analysis (Results and Discussion)

2.5.1 SPME-Isothermal GC

Solid phase microextraction (SPME) is a versatile method that combines sampling and sample introduction for GC. Its application to high speed separation has been successfully implemented.[74] Since little solvent exists during sample introduction into the GC, a 0.75 mm i.d. inlet liner was used in order to minimize the sample plug width.

Figure 2.1 shows a typical chromatogram obtained using a PDMS/DVB coated fiber. It is apparent that the general elution problem associated with isothermal GC exists in this chromatogram, because the later eluting analytes have greater peak widths although they have good peak shapes. Co-elution is a problem because the early eluting compounds have similar retention values. The software being developed for this application is designed to differentiate these components even though they overlapped greatly.

Equation (2.1) can be used to understand the various ways to increase sensitivity. Since $V_s >> \kappa_{fs} V_f$, equation (2.1) can be simplified to

$$n_f = \kappa_{fs} V_f C_0 \quad (2.3)$$

From equation (2.3), the sensitivity can be increased by increasing the volume of the fiber coating by increasing either the coating length or its thickness or both, and/or increasing κ_{fs}, the partition coefficient. Increasing κ_{fs} can be accomplished by (a) changing the fiber coating so that the coating has a higher affinity for the targeted analytes, (b) increasing the sample temperature during sampling and, (c) saturating the sample with salt. Mixing the sample (stirring, shaking, etc.) during extraction does not change any physical or chemical properties of the extraction; it merely helps to shorten the equilibrium time.

2.5.2 Optimization of Conditions

Two fibers were selected to use in this experimental design: carboxen/ polydimethylsiloxane (CAR/PDMS) and carbowax/divinylbenzene (CW/DVB). The conditions evaluated were concentration, absorption method, exposure time and desorption time. The results are listed in Table 2.3. The response variables determined are: (a) the number of peaks identified, (b) the average correlation matches of the peaks identified with the National Institute of Standards and Technology (NIST) library, and (c) the length of time until the last peak is eluted.

It can be seen from Table 2.3 that there is no easily observable difference in how many components can be identified when considering both the number of peaks and the correlation. For example, in run 5, 14 peaks were identified, however, the correlation was low, making it difficult to positively identify the compounds of interest. In runs 9 and 10, only 9 peaks were detected, however, the correlations were much higher.

Although responses listed in Table 2.3 show a higher degree of consistency across the experimental conditions, it is important to check for persistent statistical differences

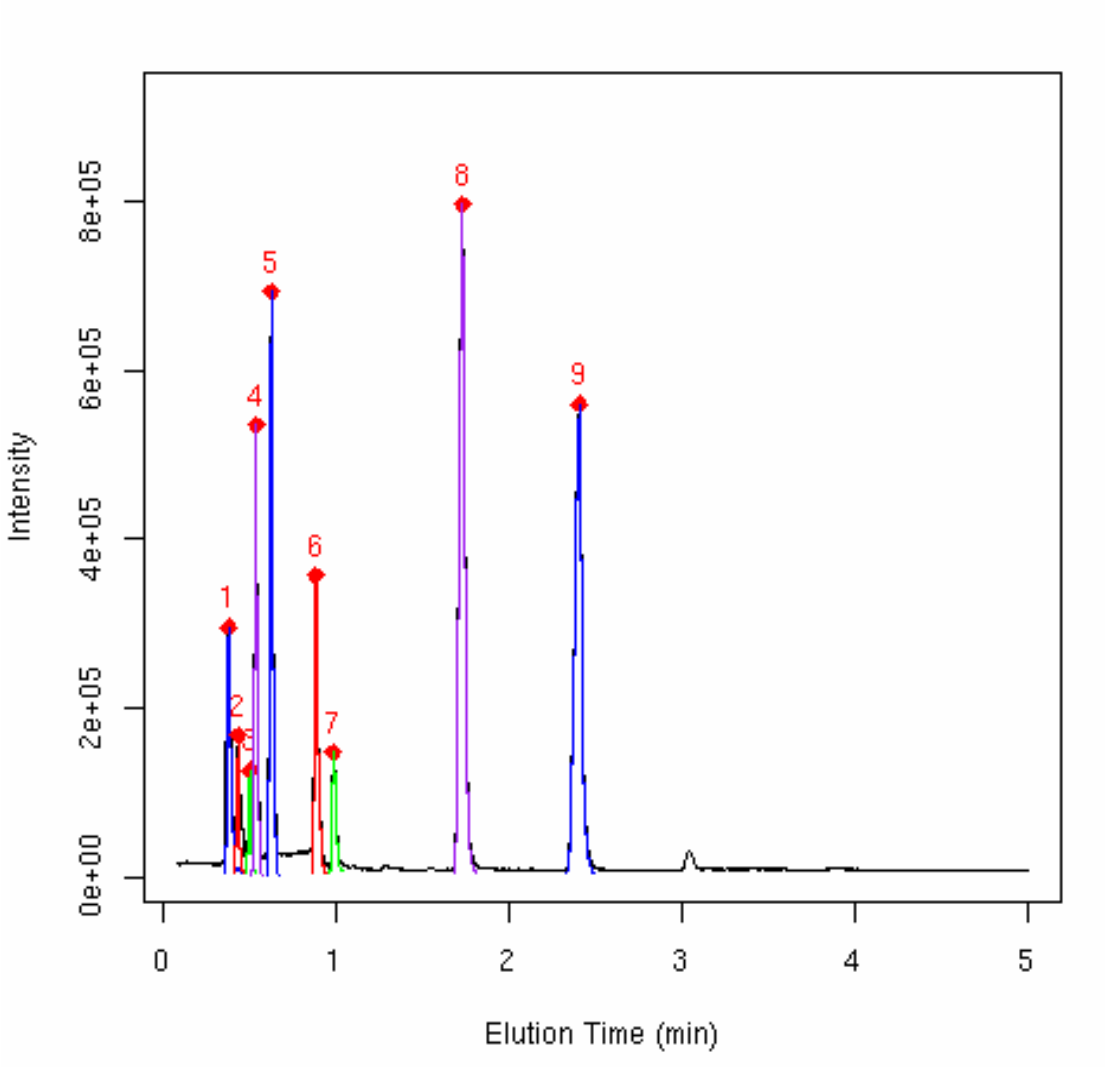

Figure 2.1 SPME-isothermal GC for selected compounds (Total Ion Chromatogram (TIC)). Conditions: 1 min extraction (direct immersion) using PDMS/DVB fiber, DB-5 column, split/splitless injection at 250 ˚C, 0.5 min desorption time with the split vent closed, oven held at 150 ˚C, MSD with a scan range of m/z = 45-200.

Table 2.3 Observed results from evaluation of the SPME with respect to operating conditions.

User	A	A	B	B	B	B	A	A	A	B	B	A
Fiber type	CAR/ PDMS	CW/ DVB	CW/ DVB	CW/ DVB	CW/ DVB	CAR/ PDMS	CAR/ PDMS	CW/ DVB	CW/ DVB	CAR/ PDMS	CAR/ PDMS	CAR/ PDMS
Sample	Dilute	Dilute	Conc.	Dilute	Comc.	Dilute	Conc.	Conc.	Dilute	Conc.	Dilute	Conc.
Exposure time (min)	8	2	8	2	8	2	8	2	8	2	8	2
Mixing method	Stir	Stir	Stir	Stir	Static	Static	Stir	Static	Static	Stir	Static	Static
Desorption time (min)	1	1	1	5	1	1	5	5	5	5	5	1
Run order	9	4	6	7	3	2	10	12	8	11	5	1
Peaks identified	10	10	12	10	14	10	12	13	9	9	11	10
[a]Correlation	0.828	0.875	0.846	0.842	0.805	0.805	0.870	0.872	0.897	0.895	0.820	0.801
[b]Time	13.35	13.61	13.81	13.52	13.70	13.40	13.64	13.65	13.62	13.38	13.34	13.34

[a]Correlation = average of the percentage match with the NIST library.
[b]Time = time needed for the last component to elute (in minutes).

across levels of the individual factors. The Plackett-Burman design allows us to examine the effects of each of these factors statistically under the assumption of no interaction. Table 2.4 lists the estimated effects of each of these factors (column 2) when the response is the peak correlation with the NIST library. Column 3 is the coefficient associated with the effect. For example, the coefficient for operator is 0.0065. This means operator A adds 0.0065 to the correlation measured while operator B subtracts that amount. Column 6 gives the P-value for the hypothesis that the coefficient could be zero. A large P-value, e.g., P>0.05, indicates that the coefficient is probably zero, meaning there is no difference in operators. The effects of all of the conditions on the response analyzed using Minitab software are listed in Table 2.4.

Usually a smaller P-value in the table indicates greater significance of the factor. The p-value for a factor should be as low as 0.01 (and even as low as 0.001) to be considered a highly significant factor. The data in the table do not contain such low numbers, which means that the tested factors have little effect on the response. However, the choice of fiber and the exposure time are more pronounced. This can be explained by considering that different fibers have different mechanisms of absorbing (adsorbing) and have different affinities for analytes. Thus different peak numbers and correlations result. Based on the equilibrium equation (2.3), the amounts of analyte absorbed (adsorbed) is related to the original sample concentration if the partition coefficient and the volume of the fiber are constant. The higher the concentration, the higher the sensitivity, which means a high correlation number. If the fiber reaches equilibrium, the exposure time and stirring will have no effect on the response. As for the desorption time, the temperature must be hot enough in order to obtain a short injection plug, which is favorable for

Table 2.4 Effects of conditions on the product of the number of peaks and correlation with the NIST library.

Term	Effect[a]	Coef[b]	SE coef[c]	T[d]	P[e]
Constant		9.1547	0.3367	27.19	0.000
Operator	0.0130	0.0065	0.3367	0.02	0.985
Fiber	1.0243	0.5122	0.3367	1.52	0.189
Sample	-1.4450	-0.7225	0.3367	-2.15	0.085
Exposure	0.7690	0.3845	0.3367	1.14	0.305
Stirring	-0.2770	-0.1385	0.3367	-0.41	0.698
Desorp	0.1387	0.0693	0.3367	0.21	0.845

[a]Factors' effect on the product of the number of peaks and correlation with the NIST library
[b]Coefficient of the factors's effect on the product of the number of peaks and correlation with the NIST library
[c]Standard error of coefficient
[d]T value
[e]P value

isothermal separations. The ideal inlet temperature will be discussed in Chapter 4.

2.5.3 Fiber Selection

The fiber selection goal was to choose a fiber that could absorb (adsorb) as many compounds as possible on our list. Twenty-four standard test compounds were dissolved in methanol and diluted in water, no salt was added, and the pH was adjusted, which means that no additional tools were used to favor absorption (adsorption). The results indicated that the PDMS/DVB fiber was slightly better to use because more compounds could be absorbed with it than any of the other commercially available fibers. However statistical analysis of the designed experiment indicated that there was little or no difference in the fibers.

Chapter 3. Gas Chromatography

3.1 Background

In the early days of GC, most attention was paid to the development of simple methods in which the parameters were maintained constant during experimentation. However, the speed, volatility and polarity ranges of GC can be substantially extended by varying the conditions in the course of the experiment. It is appropriate to consider the development of new variants of GC. A variety of methods are possible depending on the means employed for moving the components of the sample mixture along the retention layer, such as the physical states of the mobile and stationary phases, the form of the sorption layer, the temperature used, etc..

The separation temperature is one of the major parameters that determines the duration of a separation, sorbent selectivity, and the spreading of the chromatographic zones. The rational use of the thermal factor considerably extends the application range of GC. By raising or lowering the temperature of the column (sorbent), it is possible to dramatically change the properties of solute distribution in the mobile-stationary phase system, both in time and in space. The importance of this factor was demonstrated by Griffiths et al.[75] during the early days in the development of gas-liquid chromatography. Griffiths' work suggested the method of temperature programming the column. This method subsequently found wide application in GC as discussed in detail by Harris and Habgood.[76]

In GC, temperature is an important parameter that must be accurately controlled in order to obtain precise results. Usually, the column is housed in a thermostated oven. The optimum temperature depends on the boiling point of the sample and the required

resolution. Programmed temperature GC (PTGC), in which the temperature increases continuously or in steps as the separation proceeds, is usually preferred, especially for samples with a broad range of boiling points. PTGC has several advantages over isothermal conditions: (a) faster analyses can be obtained, (b) the general elution problem, which states that "the longer the compounds stay in the column, the broader the peak width," can be minimized, and (c) mixtures containing compounds of wide volatilities can be separated.

During the past several decades, there has been an increasing interest in miniaturizing field portable chromatographic systems for rapid detection and identification of hazardous chemicals, such as chemical warfare agents and their simulants and interferents. Much work has been done on the miniaturization of GC-MS because of its high resolving power and confirmative information.

Several processes contribute to total GC analysis time, including sample preparation, sample introduction, separation, detection, and cool down and re-equilibration time. Of these processes, sample preparation, separation, and cool down and re-equilibration contribute most to the analysis time. Discussion of sample preparation and introduction can be found in other chapters.

The idea of fast GC was proposed by Golay.[77] Several approaches are used to increase the speed of the GC analysis, including using a higher carrier gas flow rate, fast temperature programming, lighter carrier gas (such as hydrogen), and vacuum outlet conditions. Other researchers use short columns, thinner stationary phase films and isothermal operation for fast separations. Isothermal analysis provides the fastest overall analysis times for simple mixtures of solutes with similar volatilities.[78] Desty et al.[79]

illustrated the idea by separating more than 10 peaks in less than 2 s in a 1.2 m × 34.5 μm i.d. column with hydrogen as carrier gas under isothermal conditions. Other chromatographers have taken advantage of isothermal conditions and performed separation at high speed.[80-87] Cramers et al. showed a separation of 9 peaks in approximately 0.7 s using a 30 cm x 50 μm i.d. column with helium as the carrier gas.

There are several advantages of using the isothermal mode of separation. No cool down and re-equilibrium time is needed since the analysis is performed under isothermal conditions. This conserves power and is easy to perform. The problem with isothermal operation is that with the longer separation time, the general elution problem is more pronounced when the analytes cover a wide range of distribution constants. Since we are developing a hand-held device for fast analysis (our target separation time is within 3 min), band broadening is not a significant problem. Our main problem is how to interpret the highly overlapped GC-MS data.

3.2 Fitted Equations

The original Kováts retention indices[88] as introduced by Kováts are determined relative to a series of homologous n-hydrocarbons under isothermal conditions. For a given component *i* at a given temperature *T*, the Kováts retention index is as follows

$$I(i) = 100z + 100 \bullet \frac{\log t_R(i) - \log t_R(z)}{\log t_R(z+1) - \log t_R(z)} \qquad (3.1)$$

In temperature-programmed GC, the simple expression of elution behavior as retention relative to an arbitrary standard is not applicable, and the logarithmic relationship which exists under isothermal operation between n-alkane carbon number and retention is replaced by the approximately linear relationship:[42]

$$I = 100 \bullet \frac{t_{R(subs)} - t_{R(C_z)}}{t_{R(C_{z+1})} - t_{R(C_z)}} + 100z \qquad (3.2)$$

where $t_{R(subs)}$ is the retention time of the substance for which the retention index is to be determined, $t_{R(Cz)}$ and $t_{R(Cz+1)}$ are the retention times for the n-alkane standards, and z is the number of carbon atoms in the n-alkane standard that elutes immediately prior to the substance of interest.[89] Theoretically, each component in a mixture exhibits different characteristics which will depend on its chemical and physical properties and, thus can be separated from other components in the mixture.

The Kováts retention index has been widely used for unknown compound identification, yet the most reproducible and accurate results can be obtained under isothermal conditions. It is difficult to predict accurately retention values when dealing with temperature programmed GC, because in temperature programmed GC, not only the temperature profile but the carrier gas flow rate and column parameters, such as column dimensions and film thickness, play important roles. Considerable work[90-93] has been done to predict retention times and peak widths in temperature programmed GC using retention data measured under isothermal conditions.

Curvers et al. [94] developed a method to convert isothermal retention index data into temperature programmed data using thermodynamic parameters. Since the changes of entropy and enthalpy of each component in the separation are heavily dependent on the column dimensions, stationary phase properties and carrier gas parameters, Guan et al.[95] proposed a method described below utilizing the Kováts retention indices at two temperatures for predicting the retention values for the linear temperature programmed mode for a given column, regardless of the previously mentioned parameters.

Based on the Kováts retention index equation (3.1), since

$$k = {t_R}/{t_0} \tag{3.3}$$

substituting equation (3.3) into (3.1) and converting it into a natural logarithm, we obtain

$$I = 100z + 100\frac{\ln k - \ln k(z)}{\ln k(z+1) - \ln k(z)} \tag{3.4}$$

We can rewrite equation (3.4) as

$$\ln k = \frac{(I - 100z)}{100}\left[\ln k(z+1) - \ln k(z)\right] + \ln k(z) \tag{3.5}$$

Based on the equation

$$\ln k = \ln\frac{\alpha}{\beta} + \frac{\Delta H}{RT} \tag{3.6}$$

where I is the retention index of a certain component of interest, k is the retention factor of the component, z is the number of carbon atoms in the n-alkane eluting just before the component of interest, α is $\exp(\Delta S / R)$, β is the column phase ratio, R is the universal gas constant, ΔS is the change of molar entropy and ΔH is the change of molar enthalpy of the component. Both $\ln\frac{\alpha}{\beta}$ and ΔH can be obtained by plotting $\ln k$ versus the reciprocal of the absolute temperature and measuring the intercept and the slope, respectively. The entropy change and enthalpy change of the two n-alkanes can be obtained under two different temperatures and the retention values can be derived from the well defined equation[94]

$$\int_{T_0}^{T_R} \frac{dT}{t_0(T)\left[1 + \frac{\alpha}{\beta}\exp(\frac{\Delta H}{RT})\right]} = r \tag{3.7}$$

where T_0 and T_R are the initial temperature and the temperature at which the component of interest elutes, and r is the programming rate (˚C/min).

The prediction of retention time has been treated by Snijders et al.[93] based on the principles described above, and is described as follows

$$t_R = t_M(1+k) = \frac{L}{u}(1+k) \tag{3.8}$$

and

$$\Delta t = \frac{\Delta L_x}{u_x}(1+k_x) \tag{3.9}$$

Thus,

$$t_R = \sum_{x=1}^{n} \Delta t \tag{3.10}$$

and the peak width can be predicted the same way as above

$$\sigma_t^2 = \frac{HL(1+k)^2}{\overline{u^2}} \tag{3.11}$$

$$\sigma_{L,x}^2 = \frac{\sigma_{t,x}^2 u_x^2}{(1+k_x)^2} \tag{3.12}$$

$$\sum \sigma_{L,x}^2 = \left(\sum \sigma_{L,x}^2 \right) \frac{p_{x-1}^2}{p_x^2} + H_x \Delta L \tag{3.13}$$

$$H_{x,th} = \frac{2D_{G,x}}{u_x} + \frac{f(k_x) d_c^2 u_x}{D_{G,x}} + \frac{2k_x d_f^2 u_x}{3(1+k_x)^2 D_{L,x}} \tag{3.14}$$

$$f(k_x) = \frac{1 + 6k_x + 11k_x^2}{96(1+k_x)^2} \tag{3.15}$$

$$D_{L,x} = \frac{D_{G,x}}{5 \times 10^4} \tag{3.16}$$

$$H_x = H_{x,,th} / CE \tag{3.17}$$

$$p_x = \sqrt{P^2 - \frac{z}{L}(P^2 - 1)} \text{ where } P = \frac{p_i}{p_o} \tag{3.18}$$

The total peak width can be rewritten as

$$\sigma_t^{\,2} = \frac{\left(\sum_{x=1}^{n} \sigma_{L,x}^2\right)(1 + k_n)^2}{u_n^2} \tag{3.19}$$

where L is the column length, CE is the coating efficiency, $H_{x,th}$ is the theoretical plate height (H_x is the local plate height, and is equal to $H_{x,th}$ when CE is 100%), d_c and d_f are the column i.d. and film thickness, respectively, p_i and p_o are the gas pressures at the inlet and outlet of the column, respectively, p_x is the pressure at any position z, u_x is the linear velocity of the analyte at the xth segment, ΔLx is the distance the analyte travels in time Δt, and is equal to the length of the column segment, and $D_{l,x}$ is the diffusion coefficient of the analyte in the stationary phase.

Attention should be paid to pressure, because with an increase in temperature, the viscosity changes. Also the compressibility of the carrier gas plays an important role in its linear velocity. Attention also should be paid to the numerical steps which are used in all of the equations mentioned above. Only if the time intervals or the segments are chosen to be small enough, can the retention factors and the carrier gas velocity be assumed constant. In order to ensure calculation accuracy, it is estimated that the time interval of the integration should be less than 0.005 t_0.[96]

3.3 Experimental

3.3.1 Chemicals

All of the chemicals from Table 1.1 were dissolved directly in anhydrous methyl alcohol. The concentration of each component is listed in Table 3.1. In this study, the test

Table 3.1. Sample concentrations used in this study.

No.	Name	Amount added (μL)	Conc (v/v)[a] $\times 10^{-3}$
1	Isopropanol	15	1.9
2	Ethyl acetate	10	1.25
3	Isobutyl alcohol	5	0.63
4	Ethylene glycol	10	1.25
5	Pinacolyl alcohol	5	0.63
6	Toluene	5	0.63
7	Dimethyl formamide	5	0.63
8	Dimethyl sulfoxide	10	1.25
9	4-Hydroxy-4-methyl-2-pentanone	5	0.63
10	Chlorobenzene	5	0.63
11	Dimethyl methylphosphonate	8	1.0
12	2-Methyl-2,4-pentanediol	8	1.0
13	2-Chlorophenol	5	0.63
14	1-methyl-2pyrrolidone	10	1.25
15	Diethyl malonate	5	0.63
16	Triethyl phosphate	6	0.75
17	2,2-Thiodiethanol	6	0.75
18	Methyl salicylate	6	0.75
19	Chloroacetophenone	0.00824 g	1.03 (g/mL)
20	Isoamyl salicylate	8	1.0
21	Chlorobenzylidene malononitrile	0.00798 g	1.00 (g/mL)
22	Diethyl phthalate	6	0.75
23	Tributyl phosphate	6	0.75
24	Parathion	6.5	0.81

[a]All of the chemicals were dissolved in anhydrous methyl alcohol at a concentration of ~1000 ppm.

sample was prepared by dissolving a set of standard compounds into anhydrous methyl alcohol to a concentration of about 1/1000 (vol/vol) each. The solution was then diluted with de-ionized water to the ppm level. A 2-mL fresh solution was used for each extraction. A 5.1 m × 50 μm i.d DB-5 column with 0.2 μm film thickness (Agilent, Wilmington, DE) was used. Helium was used as carrier gas with a flow rate of 22 cm/s.

3.3.2 Instrumentation

A Fisons-8000 model GC (Thermo Finnigan, San Jose, CA) with an FID detector was used. E-Z Chrome software was used to collect data. Rtx-5Sil MS columns were purchased from Restek (Bellefonte, PA) and DB-5 columns were purchased from Agilent (Palo Alto, CA). Linear gas velocities of 17 cm/s and 34 cm/s were used, and the injector and detector temperatures were maintained at 250 ˚C and 280 ˚C, respectively. The column oven temperature was increased linearly from 30 ˚C to 230 ˚C at a rate of 4˚C/min.

3.4 Results and Discussion

3.4.1 Theoretical Study

In order to investigate the effect of temperature on elution time, five compounds were randomly selected from the list of simulants and interferents, covering the whole range of retention indices of the compounds of interest. These five are listed in Table 3.2.

Figure 3.1 shows some of the results of the five selected compounds run under isothermal conditions at different temperatures. From this figure, it is easy to see that the linear velocity increases with increasing temperature. This can be understood by referring to retention theory starting with

$$\bar{\upsilon} = \frac{L}{t_R} \tag{3.20}$$

Table 3.2 Properties of five compounds that cover the range of retention indices of interest.

	MW[a]	MP (˚C)[b]	BP (˚C)[c]	Retention Index
Isopropanol	60.1	-88.5	82.4	483
Chlorobenzene	112.6	-45.6	130	850
Methyl salicylate	152.1	19.4	220-224	1193
Tributyl phosphate	266.3	-80	289	1616
Parathion	291.3	6.1	375	1942

[a]molecular weight
[b]melting point
[c]boiling point

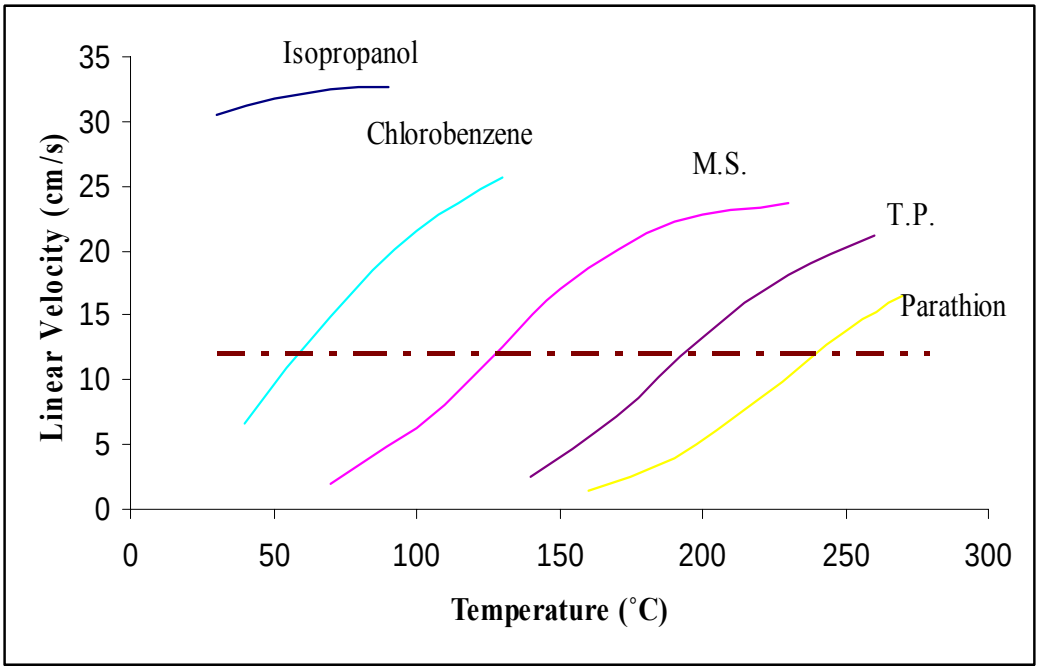

Figure 3.1. Change in linear velocity of selected compounds as a function of temperature. M.S. is methyl salicylate and T.P. is tributyl phosphate. The dashed line describes the temperature difference if all the component have the same linear velocity.

and

$$u = \frac{L}{t_M} \tag{3.21}$$

where L is the length of the column, $\bar{\upsilon}$ is the average linear velocity of the analyte, u is the linear velocity of the mobile phase, and t_R and t_M are the retention time and the dead time of the analyte, respectively. If partitioning (the distribution of analytes between the stationary phase and mobile phase) can be considered to be a "dip in and out" process, we can express the migration rate as a fraction of the velocity of the mobile phase, and $\bar{\upsilon}$ equals u times the fraction of time an analyte spends in the mobile phase.

The fraction of time is equal to the average number of moles in the mobile phase divided by the total number of moles at any instant. Thus,

$$\bar{\upsilon} = u \times (\text{number of moles in the mobile phase/total number of moles}) \tag{3.22}$$

We can rewrite equation (3.22) as

$$\bar{\upsilon} = u \frac{c_M V_M}{c_M V_M + c_S V_S} \tag{3.23}$$

where c_M and c_S are the concentrations of analytes in the mobile and stationary phases, respectively, and V_M and V_S are the volumes of the mobile and stationary phases, respectively. The equation also can be rewritten as

$$\bar{\upsilon} = u \Big/ \left(1 + c_S V_S \Big/ c_M V_M\right) \tag{3.24}$$

For a certain separation, if the velocity, column and temperature are set beforehand

$$V_S \Big/ V_M = K \tag{3.25}$$

where K is a constant and

$$\bar{\upsilon} = u \Big/ \left(1 + K\frac{c_S}{c_M}\right) \tag{3.26}$$

Based on Henry's law, i.e. "the concentration of a solute gas in a solution is directly proportional to the partial pressure of that gas above the solution," c_S/c_M is constant at a defined temperature. It should be noted that the restricted condition of "ideal dilute solution" may not be true in this case. From equation (3.26), we can easily conclude that under certain conditions, such as a particular column and temperature, the elution time remains the same. This is one way to use retention indices to confirm the identities of unknown compounds when nonspecific detectors, such as the FID, are used.

Another phenomenon seen in Figure 3.1 is that the linear velocities of analytes approach zero with decreasing temperature and plateau with increasing temperature. This can be explained by equation (3.26). Since the heat or enthalpy change of the dissolution reaction of most compounds is negative, the solubility of gases generally decreases with increasing temperature; therefore, c_M increases and c_S decreases with an increase in temperature, and c_S/c_M approaches zero when the temperature is higher than the boiling point of the analyte of interest. The average linear velocity of the analyte becomes closer to the linear velocity of the carrier gas, and becomes identical when the temperature is high enough because the linear velocity decreases linearly with an increase in temperature (data not shown). Accordingly, c_S/c_M approaches infinity when the temperature is less than the melting point of the analyte.

Another interesting fact from Figure 3.1 is that different analytes can be eluted out of the column at a constant rate in a single column if each is exposed to a different specific temperature (dashed line). Suppose that the column is heated differently along the column. Then, the separation can be affected by additionally moving the temperature

gradient along the column (i.e., the column temperature varies lengthwise with time, as opposed to simultaneously along the column as in chromatography with temperature programming),[97] which is called chromathermography. In contrast to separation under isothermal conditions, it is possible to increase the concentration of substances at the maximum of the chromatographic zone because of the focusing force the analytes encounter; this consequently provides higher chromatographic peaks and greater sensitivity. The chromathermographic method is exceptionally convenient for the separation of substances that differ greatly in their properties. (e.g., boiling point). It combines the advantages of thermal desorption and elution chromatography, and is applicable to the analysis of mixtures that contain components with both strong and weak sorption abilities, irrespective of their sorption isotherms.

3.4.2 Isothermal GC

Figure 3.2 shows a comparison of isothermal chromatograms of a mixture of simulants and interferents at different temperatures. The components in the figure are iso-amyl salicylate, diethyl phthalate, and tri-butyl phosphate. These three compounds were chosen because they can be easily distinguished. The elution time can be reduced from more than 50 min to less than 7 min by changing the temperature. Because of the high boiling points of the compounds selected, a long elution time was experienced for the components (~53 min for tri-butyl phosphate) at 130 ˚C. The effect of the general elution problem is difficult to see from the figures because the residence time for each compound in the column was long and the retention time differences were not significant. However, with an increase in oven temperature, the peak shapes became distorted and the resolution decreased. This is because of the high boiling points of the test compounds. When the

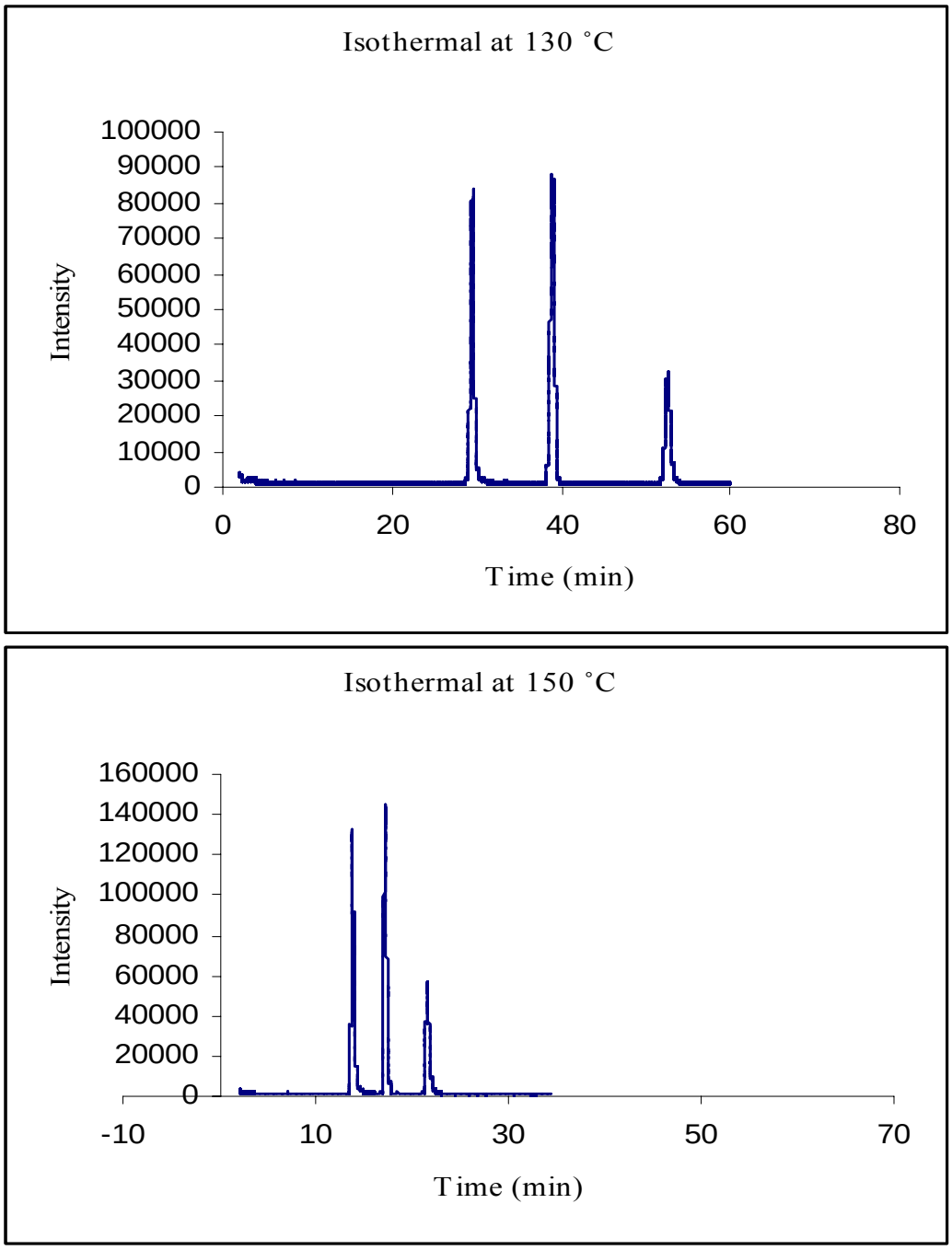

Figure 3.2 Effect of temperature on isothermal chromatograms for selected compounds. Conditions: 10 m × 100 µm i.d., 0.2 µm film thickness DB-5 column, 250 ˚C injection temperature, helium carrier gas at a flow rate of 17 cm/s.

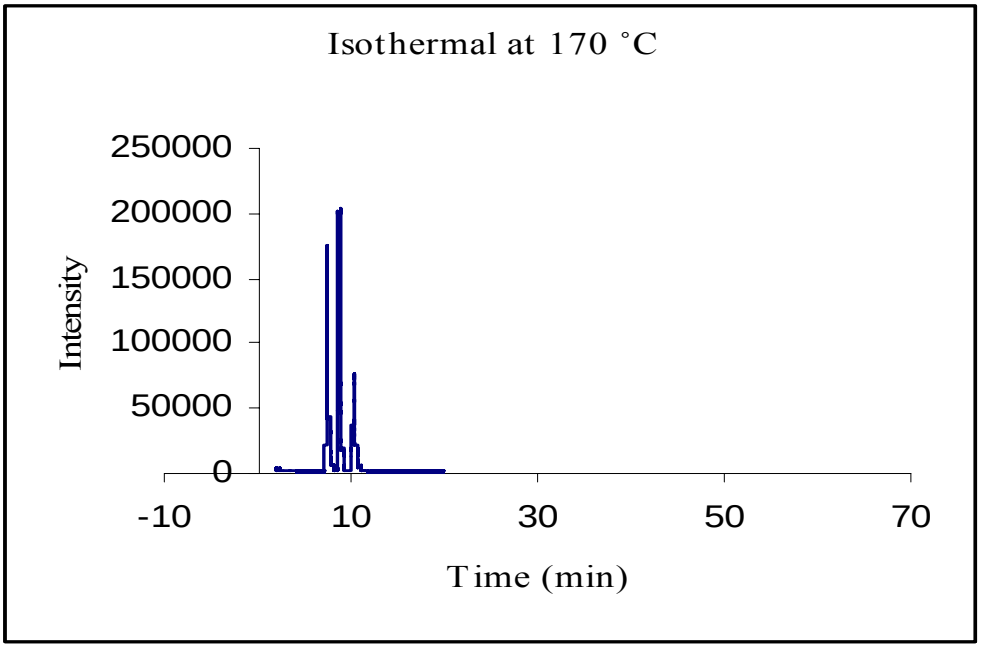

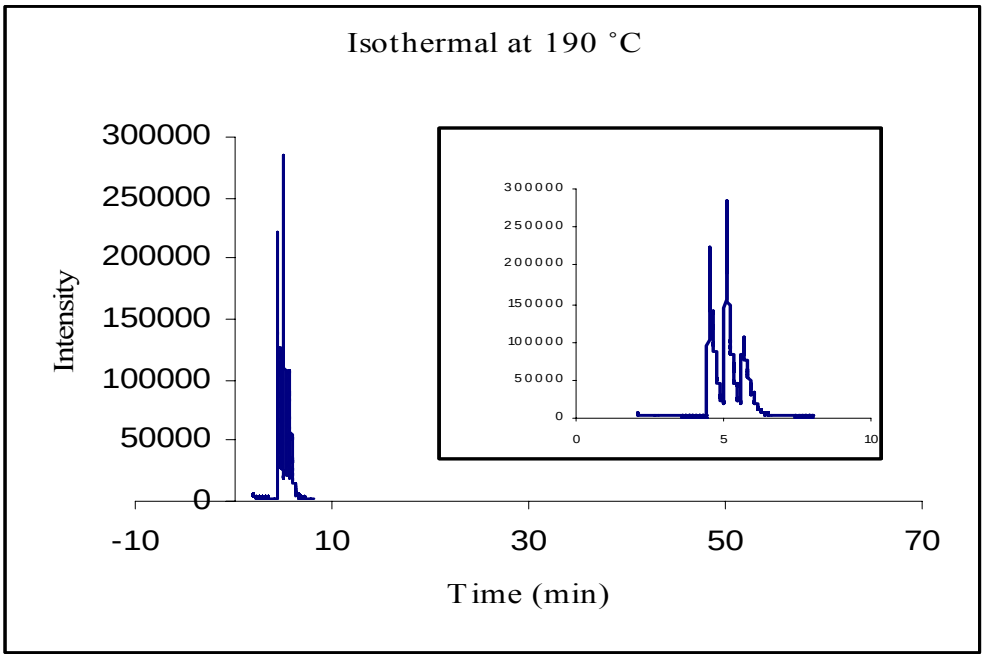

Figure 3.2 continued

column temperature is low, the vaporized sample can be focused at the head of the column and a short injection plug is formed and a narrow peak can be guaranteed. However, when the oven temperature is increased, the vapor pressures of the solutes increase and less focusing results; this results in wider peaks. Also, a higher temperature increases the diffusion coefficients of the compounds, which also contributes to broader peak widths.

The equation that governs resolution is

$$R_s = \frac{k_B - k_A}{1 + k_B} \times \frac{\sqrt{N}}{4} \tag{3.27}$$

where R_s is the chromatographic resolution, k_A and k_B are retention factors for two different compounds, and N is the plate count for the column. While the efficiency, N, is dependent on the column, mobile phase, stationary phase, and operating conditions, N in this treatment will be regarded as a constant, because all of these conditions can be predetermined. As defined, $\alpha = \frac{k_B}{k_A}$ and equation (3.27) can be rewritten as

$$R_s = \left(\frac{\alpha - 1}{\alpha}\right)\left(\frac{k_B'}{k_A'}\right) \times \frac{\sqrt{N}}{4} \tag{3.28}$$

With an increase in temperature, the difference between k values for different compounds decreases, α approaches 1, and $\left(\frac{\alpha - 1}{\alpha}\right)$ approaches zero. At the limit, no separation will occur because the temperature is too high.

Another interesting phenomenon is that the logarithm of $(V_c - V_a)/V_a$ is linearly proportional to $1/T$, the reciprocal of the oven temperature (units of Kelvin), where V_a and V_c are the linear velocities of the analyte and carrier gas, respectively, because

$$V_a = L/t_R \tag{3.29}$$

and

$$V_c = L/t_0 \tag{3.30}$$

where t_R is the time it takes the analyte peak to reach the detector, t_0 is the time for a non-retained species to reach the detector, and L is the length of the separation column.

Thus,

$$(V_c - V_a)/V_a = (t_R - t_0)/t_0 \tag{3.31}$$

Since $t_R = t_0(1+k)$, this equation can be rewritten as

$$(V_c - V_a)/V_a = k \tag{3.32}$$

Figure 3.3 shows plots of log k with respect to $1/T$ (in Kelvin) for two compounds. The relationship of k vs $1/T$ can be rewritten as

$$\log\left(\frac{V_c - V_a}{V_a}\right) = 2369.2\frac{1}{T} - 4.7076 \tag{3.33}$$

for tributyl phosphate and

$$\log\left(\frac{V_c - V_a}{V_a}\right) = 1724.1\frac{1}{T} - 3.8989 \tag{3.34}$$

for methyl salicylate.

If equations (3.33) and (3.34) are combined with equation (3.32), the two equations can be rewritten as:

$$\log k = 2369.2\frac{1}{T} - 4.7076 \tag{3.35}$$

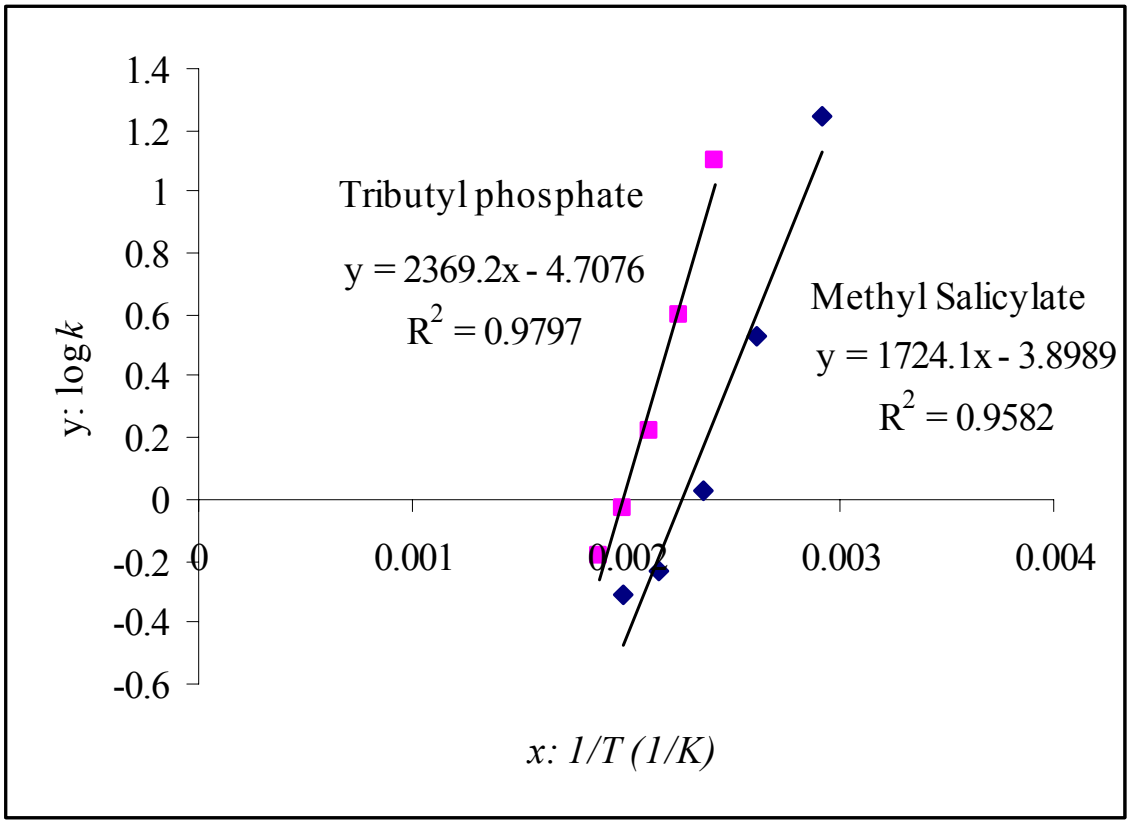

Figure 3.3 Plot of log *k* vs reciprocal of temperature *T* (in Kelvin). Conditions: Fisons 8000 GC with FID detector, 250 ˚C inlet temperature, 3 m × 250 µm i.d., 0.25 µm film thickness Restek-5Sil-MS column, helium carrier gas at a flow rate of 35.2 cm/s.

and

$$\log k = 1724.1\frac{1}{T} - 3.8989 \tag{3.36}$$

When comparing equations (3.35) and (3.36) with the van't Hoff equation, it is easy to see that they have a similar format. Thus, we can say that the process of GC separation can be described by the process of adsorption/absorption and desorption. From these equations the energy needed for tributyl phosphate or methyl salicylate to absorb (adsorb) in and desorb from the column stationary phase can be easily calculated. The distribution coefficients, *K*, as well as the retention factors and the isotherms for different compounds can then be deduced from these equations.

Another interesting observation from Figure 3.1 is that the separation time can be shortened by one half, as the oven temperature increases 15-20 ˚C. Once again, if we treat the separation process as a reaction, the van't Hoff approximation, which states that "the reaction rate increases two to four times as the temperature increases 10 K," can be applied.

Careful examination of Figure 3.3 shows that the statistically measured R^2 values for the linear fit for these equations are not as good as we expected (approaches to 1). This problem arises from sources of uncertainty in the experiment. There are several sources for uncertainty including a high level of random noise in measurement, incorrect assumptions regarding the linear model, or changes in the assumptions regarding the parameters. In the current measurement, the random noise is low. However, the assumption that the carrier gas linear velocity remains the same throughout the temperature range is demonstrated to be incorrect. We used the same flow rate at different temperatures for simplification; however, this assumption is not right since the

carrier gas linear velocity decreases linearly with increasing temperature (experimental data not shown).

Another interesting observation for dimethyl sulfoxide and chlorobenzene is that they change their elution orders depending on the elution temperature. This phenomenon can be explained by looking at Figure 3.4.

From Figure 3.4, one can see that the two lines for chlorobenzene and dimethyl sulfoxide are not parallel, and they intersect at approximately 50 ˚C. At this point, there is no separation at all; instead, the two compounds coelute. The farther the temperature is from this point, the better the resolution will be for the two compounds. More information about such a phenomenon can be found elsewhere.[98]

3.4.3 Temperature Programmed GC

The mixture of 24 simulants and interferents was run using the temperature-programming mode for comparison to the isothermal mode, and the result is shown in Figure 3.5.

Several peaks tail, including 7 (dimethyl formamide), 9 (4-hydroxy-4-methyl-2-pentanone), 11 (DMMP), 14 (1-methyl-2-pyrrolidinone), 16 (triethyl phosphate), and 23 (tributyl phosphate); this may due to interactions of these compounds with active sites on the column surface due to their polarities. Although it is difficult to separate all of the components of interest,[99] it is easy to see that most of the components are well separated. The reasons for the difficulty experienced in separating compounds such as 4-hydroxy-4-methyl-2-pentanone, dimethyl sulfoxide and chlorobenzene, were discussed previously.

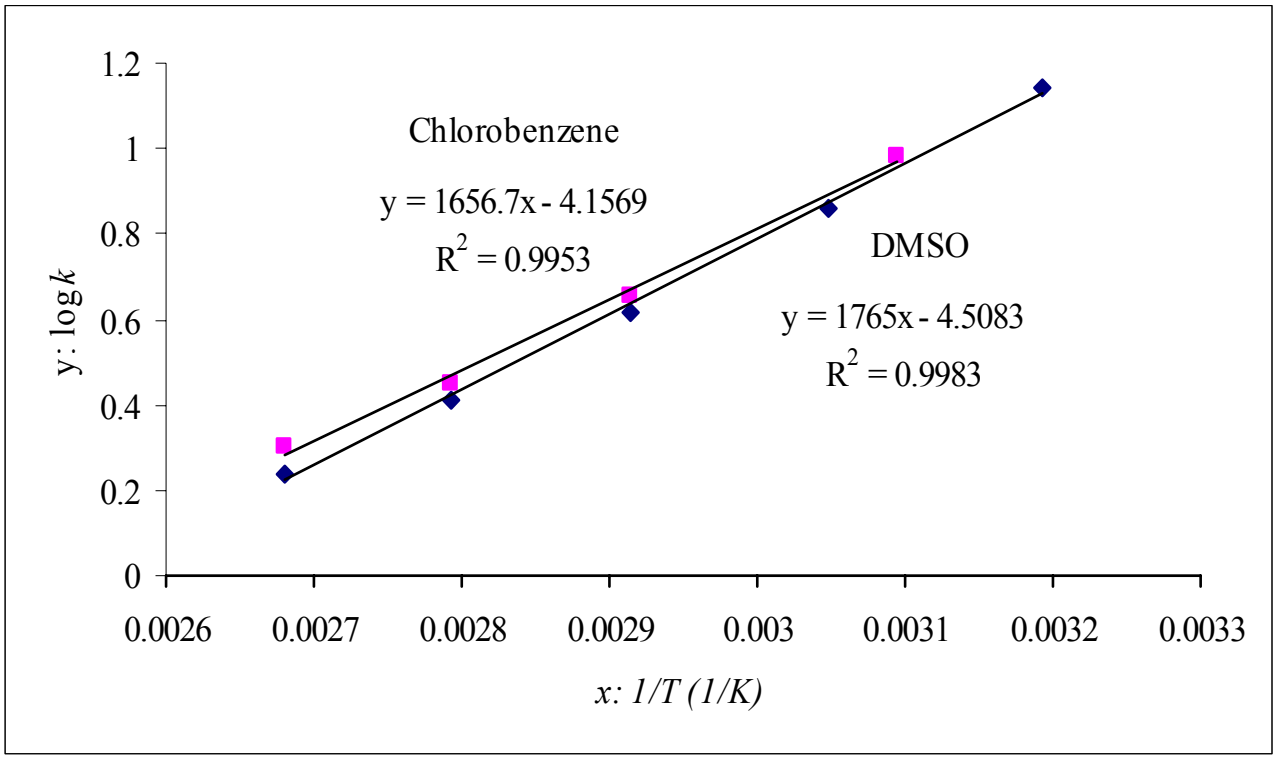

Figure 3.4 Plots of log *k* vs *1/T* for dimethyl sulfoxide and chlorobenzene. Conditions: HP 6890 GC coupled with an MSD, 10 × 100 µm i.d., 0.2 µm film thickness DB-5 column, 250 ˚C injection temperature, helium carrier gas at a flow rate of 17 cm/s.

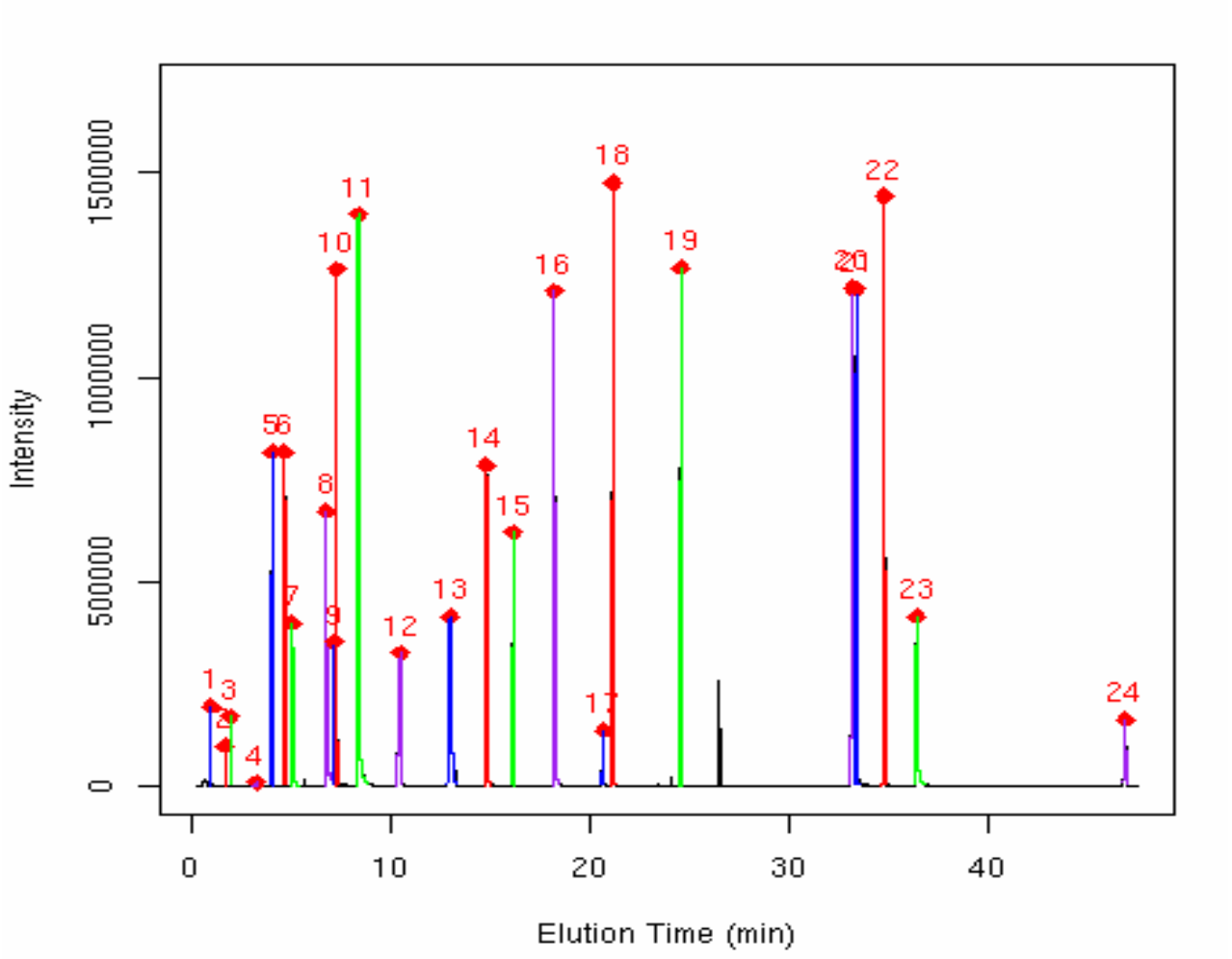

Figure 3.5. Temperature programmed chromatogram of simulants and interferents (TIC). Conditions: HP 6890 GC coupled with an HP 5973 MSD, 10 m ×100 µm i.d. DB-5 column with 0.4 µm film thickness, helium carrier gas at 52 cm/s, temperature program from 30 ˚C at 4 ˚C/min to 200˚C. The 24 compounds are listed in Table 1.1.

Chapter 4. Optimization of Conditions for Isothermal Gas Chromatography-Mass Spectrometry with Solid Phase Microextraction

4.1 Overview

The purpose of this chapter is to explain the experimental design and analysis used to optimize the GC conditions for chemical agent detection. "Optimization" means to select the column and operating conditions that give the "best" performance among the list of possible column characteristics and operating conditions. The characteristics and operating conditions considered were:

1. Stationary phase: 5%-phenyl 95%-methylpolysiloxane (DB-5) and 14%-cyanopropyl-phenyl) methylpolysiloxane (DB-1701)
2. Film thickness: 0.1 μm and 0.4 μm
3. Column length: 10 m, 5 m, and 3 m
4. Column temperature: 90 ºC to 200 ºC, depending on the length of column
5. Injection temperature: 160 ºC to 260 ºC (the highest temperature recommended by the manufacturer)
6. Head pressure: 1 psi to 30 psi, depending on the length of the column (30 psi is the highest head pressure that can be used for the Agilent 5890 II GC)

The first three variables defined the characteristics of the GC column and the last three specified the operating conditions for the GC. The optimum conditions for these variables were determined by four criteria. These were: (a) number of peaks identified for each chromatogram; (b) an eyeball evaluation (grade) for each chromatogram; (c) analysis time, and (d) average percentage match against the NIST library. A list of

optimal operating conditions was tabulated for each criterion. The final column dimensions and operating conditions were then selected from this list of optimal values.

4.2 Experimental Design

Many variables might be used to characterize the quality of the separation. An experienced chromatographer feels he/she can usually give a quick eyeball evaluation of a chromatogram. This is "real time" in the sense that information can be used immediately. In order to establish a first order check on the viability of an experiment, an eyeball assessment of each chromatogram was used as it was generated. Scores between 0% (bad) and 100% (perfect) were made. Although more sophisticated dependent variables were obtained later, this grade was like a parity check. Since this method is real time, the operator can determine the operating conditions for achieving an approximately optimal eyeball score. These optimal conditions should be close to the optimal conditions of the other criteria. These real time assessments, for example, retention time and amount of overlap, were potential dependent valuables measured to determine an optimum. Subsequent dependent variables were a peak number check and the average correlation from the de-convolution profile matching program. These subsequent analyses based on more sophisticated methods of measuring were used for two purposes. First they are used to evaluate the "eyeball" method. As the "eyeball" method is used here to determine a first order approximation, it is a useful method to approximate optimal experimental values as the experiment is carried out. The second purpose is that the other criteria yield more precise measurements that can be used to determine more explicitly optimal experimental conditions.

The sequence of experiments done to gather data for selecting the optimum column was done using a Box-Behnken type design for each column type and length. This means that for each set of stationary phase film thickness-length option evaluation (12 in all) a series of 15 experiments would be conducted. The Box-Behnken type design specifies the condition of variable settings such that both linear and quadratic main effects can be estimated. Thus, the settings of the variables for 8 of these 15 experiments represent extreme operating conditions and others represent intermediate conditions. This allows the estimation of a curved surface response which could be used to determine the optimum value. The values of the variables for the 15 experiments are given in Table 4.1.

The optimum value could be determined in "real time" using a statistical analysis program such as Minitab. If the response variable is known immediately, a prediction of the optimal setting can be made by first making an eyeball examination of the chromatogram to fit a response model. This response model gives a predicted value for the input variables to obtain the optimal eyeball examination value. To confirm this value to be optimal, a separation was performed at the proposed optimal values and the outcome was compared with the predicted value.

The data in Table 4.1 give the levels of column temperature, injection temperature and head pressure for each of the 15 runs, which were done in the order indicated. In practice, the correlation resulting from the run can be determined by the outcome of each of the experimental runs. From these runs, we could fit a model of response. We could also plot the correlation as a function of the various settings.

Table 4.1 Example of a Box-Behnken design.

# of Run	Std Order	Run Order	Oven Temp (˚C)	Inj Temp (˚C)	Head Pressure (psi)
1	1	1	90	180	2
2	15	2	110	220	2
3	4	3	130	260	2
4	9	4	110	180	1
5	3	5	90	260	2
6	5	6	90	220	1
7	10	7	110	260	1
8	12	8	110	260	3
9	7	9	90	220	3
10	14	10	110	220	2
11	8	11	130	220	3
12	2	12	130	180	2
13	13	13	110	220	2
14	6	14	130	220	1
15	11	15	110	180	3

4.3 Experimental

4.3.1 Materials

Capillary columns of 100 μm i.d., 0.1 μm and 0.4 μm film thickness, DB-5 and DB-1701, were purchased from Agilent Technologies (Wilmington, DE), Polydimethylsiloxane/divinylbenzene (PDMS) fibers were obtained from Supelco (Bellefonte, PA) and conditioned before use as recommended by the manufacturer. All chemicals used are as listed in Table 2.1, in Chapter 2. The test samples were prepared also as listed in Table 2.2.

4.3.2 Instrumentation

All experiments were performed using an HP 5890 II GC (Agilent) coupled to a Saturn II ion trap mass spectrometer (Varian, Palo Alto, CA). Statistical experimental design approach was used to determine the parameter settings for optimum response.[100] The Box and Behnken design provides a class of incomplete three level factorial designs.[101] These designs are nearly orthogonal designs that allow for estimating linear effects, quadratic effects, as well as linear 2-way interactions.[100] Unlike the central composite designs, Box-Behnken designs just use three levels of each factor, and they are more rotatable. In addition, all design levels are interior to the range of specified values; estimation of linear quadratic and interaction effects gives the ability to construct a parabolic response surface. This means that it gives a set of contour plots of the response, e.g., how good the separation is as a function of the experimental conditions. From this, the "optimal" values or experimental conditions that give the best separation can be determined even though we may not have actually run an experiment at these "optimal"

levels. The condition for selecting optimality requires the quadratic surface to be a good approximation. An additional run at the optimal value provides a test for this assumption.

4.3.3 Factorial Design

Three factors with three center points were used in the experimental design to optimize the operating procedure. The design consisted of replicated center points and a set of points lying at the midpoint of each edge of the multidimensional cube that defined the region of interest. The non-linear model (in the X's) generated by the design is of the form

$$Y = A_o + A_1X_1 + A_2X_2 + A_3X_3 + A_4X_1X_2 + A_5X_2X_3 + A_6X_1X_3 + A_7X_1^2 + A_8X_2^2 + A_9X_3^2 + E \quad (4.1)$$

In this model Y is the measured response (one of the criteria detailed above) associated with each factor-level combination, A_o is an intercept, A_1-A_9 are the regression coefficients, E is the error term,[101] and X_1, X_2 and X_3 are the factors studied. Three independent variables are listed in Table 4.2, which are injection temperature, oven temperature and column head pressure.

4.4 Results and Discussion

In this experimental design, two different stationary phases, DB-5 and DB-1701, with two different film thicknesses were evaluated. The DB-5 column can be regarded as non-polar and DB-1701 as mid-polar. Different lengths of the column were also studied, i.e., 3, 5, and 10 m. Obviously, the longer the column, the better the separation would be expected. However, a longer column requires longer analysis time and/or higher electrical power if shorter time is desired. Shorter columns are typically used for fast analysis.

Table 4.2 List of the column characteristics and the operating conditions used in the factorial design.

Column type	Film thickness (μm)	Column length (m)	Injection temp (˚C)	Oven temp (˚C)	Head pressure (psi)
DB-5	0.4	10	200~250	150~200	15~30
		5	180~260	110~150	5~15
		3	180~260	90~130	1~5
DB-5	0.1	10	160~260	150~200	15~30
		5	180~260	110~150	5~15
		3	180~260	90~130	1~5
DB-1701	0.4	10	200~250	150~200	15~30
		5	180~260	110~150	5~15
		3	180~260	90~130	1~5
DB-1701	0.1	10	160~260	150~200	15~30
		5	180~260	110~150	5~15
		3	180~260	90~130	1~5

Based on a Box-Behnken design, fifteen experiments were required for the response to be determined. A total of 180 experiments were done for the 12 sets of experimental designs. Each chromatogram was eyeball evaluated and a score was given based on the peak shapes, number of peaks identified, resolution, and identifiability of each compound. These values were fitted immediately to a model, and the optimal values of the experimental variables were obtained. The last experiment for each set was done at the optimal values. The chromatograms were subsequently de-convolved using the software[102] developed in the laboratory to determine correlation with the NIST library.

The response for each run was based on the number of identifiable peaks, the average correlation coefficient, the eyeball evaluation grade, and the reciprocal of $(10+t_R)$, where t_R is the retention time of the least volatile component in the mixture (in this case, chloroacetophenone). Time was counted here because our goal was to achieve fast analysis. The time needed for the runs was as long as 25 min and as short as one min. In order to reflect the correct effect of time on analysis, a constant 10 was added to the retention time, and its reciprocal was used since the longer the time, the smaller the response. We then select operating conditions to maximize the reciprocal.

Most of the designs showed basically the same results determined from any of the response factors. For example, the advantage of shortened analysis time can be offset by the grade of the chromatogram and the peak numbers identified; a larger number of identified peaks and a higher grade could be offset by the longer analysis time needed, and vice versa. However, when the responses were investigated in detail, two experimental designs showed comparatively higher scores than all others. One experimental design was for the 3 m DB-5 column (0.1 μm film thickness). The other

was for the 5 m DB-1701 column (0.4 μm film thickness). For these two experimental designs, the results are listed in Tables 4.3 and 4.4.

The mathematical relationship in the form of a fitted polynomial equation for the measured responses was obtained using Minitab. The polynomial equation relating to the response with the independent variables was

$$Y=50.543+9.629X_1-7.690X_2+7.239X_3-3.422X_1^2+5.551X_2^2$$
$$-2.357X_3^2+4.328X_1X_2+3.975X_1X_3-0.223X_2X_3. \quad (5.2)$$

A negative sign indicates a negative effect, a positive sign indicates a positive effect, while the whole equation represents the quantitative effects of the independent variables and their interactions on the response. This was not the case here because all of the factors did not quantitatively affect the response. In our case, only a trend was shown and exact parameters still need to be confirmed through experiments.

The relationship of the response and independent factors can be elucidated by the contour and surface plots shown in Figures 4.1 and 4.2, in which it is easy to see the trends for optimizing the operational conditions. In order to obtain high performance, the analysis needed to be done under the optimized conditions. The figures show that the higher the head pressure, the better the results. This is actually not true because there is an optimal carrier gas linear velocity, which for helium is approximately 25-40 cm/s.

Another observation is that the lower the oven temperature, the better the resolution. However, the analysis time is longer and the eyeballed grades are low because of the general elution problem. The higher the oven temperature, the greater the overlap of closely eluting compounds, and a compromise must be made. In this experimental design, the higher the inlet temperature, the better the results. We performed several extra

Table 4.3 Observed responses for 3 m DB-5 column with 0.1 μm film thickness.

Run order	Injection temp (X1)	Oven temp (X2)	Head pressure (X3)	Peaks identified	Average correlation	Eyeball grade	$1/(10+t_R)$	t_R	Response (Y)
5	260	90	2	13	0.839	80	0.0743	3.45	0.810
13	220	90	3	13	0.850	80	0.0757	3.22	0.837
15	260	110	3	12	0.846	78	0.0863	1.58	0.876
7	220	110	2	12	0.824	65	0.0854	1.72	0.845
8	220	110	2	12	0.820	60	0.0855	1.70	0.841
14	220	130	3	8	0.896	78	0.0912	0.97	0.654
3	220	130	1	8	0.877	65	0.0900	1.12	0.631
11	180	90	2	12	0.831	75	0.0745	3.42	0.743
2	220	90	1	13	0.789	75	0.0729	3.72	0.748
9	220	110	2	10	0.835	65	0.0854	1.72	0.713
10	180	130	2	8	0.876	50	0.0908	1.02	0.636
1	180	110	1	8	0.855	45	0.0840	1.90	0.575
6	260	130	2	10	0.802	80	0.0908	1.02	0.728
12	180	110	3	10	0.838	55	0.0862	1.60	0.722
4	260	110	1	11	0.803	56	0.0846	1.82	0.747

Table 4.4 Observed response of additional experiments for optimizing the operational conditions.

Run order	Injection temp (X1)	Oven temp (X2)	Head pressure (X3)	Peaks identified	Average correlation	Eyeball grade	$1/(10+t_R)$	t_R	Response (Y)
1	260	90	3	14	0.814	75	0.0761	3.13	0.867
2	180	90	3	12	0.827	72	0.0757	3.22	0.751
3	180	90	1	12	0.804	69	0.0731	3.68	0.705
4	220	90	1	12	0.842	72	0.0729	3.72	0.737
5	220	90	2	14	0.800	78	0.0741	3.50	0.830

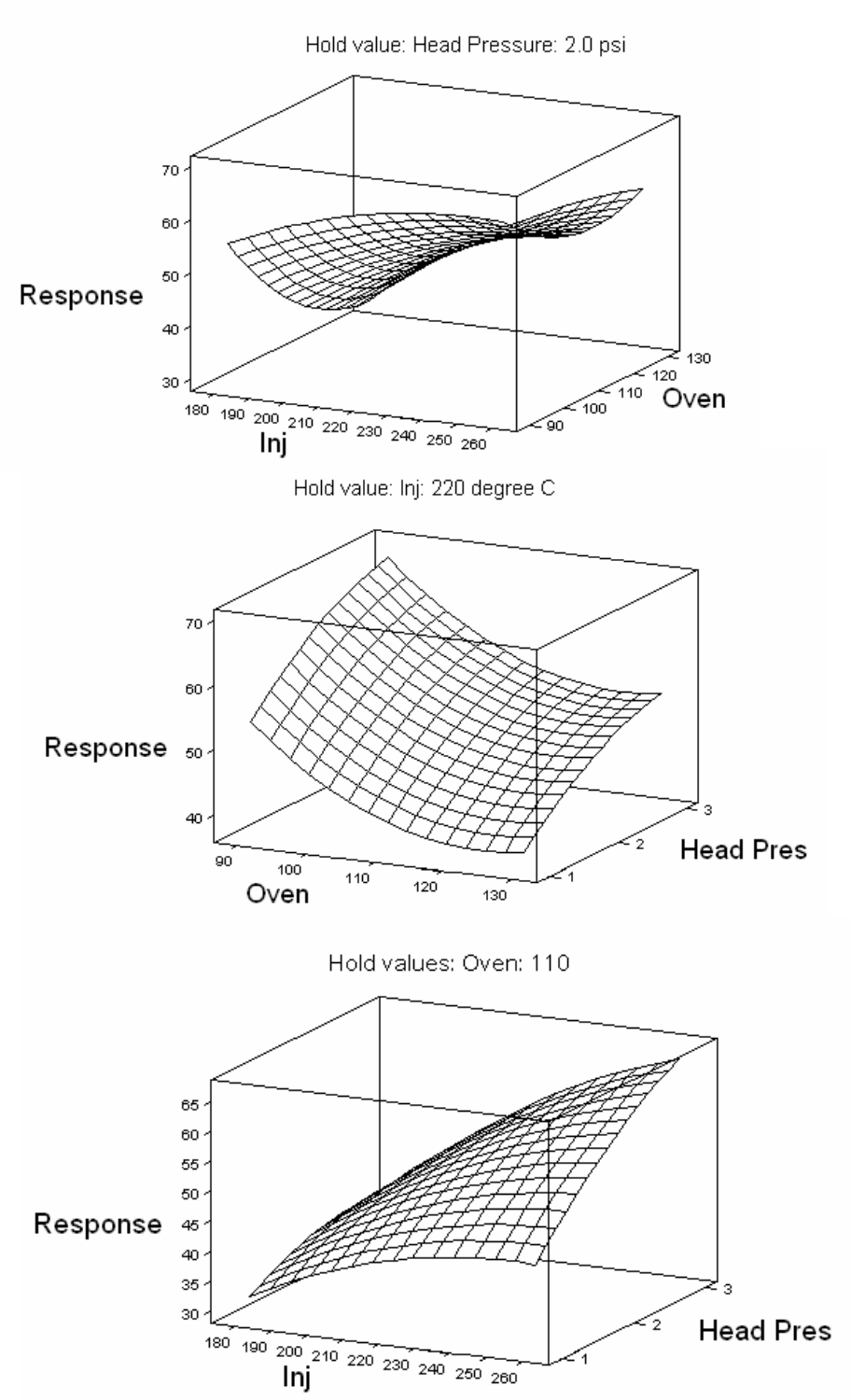

Figure 4.1 Surface response plots showing the effects of injection temperature, oven temperature and head pressure for DB-5 column.

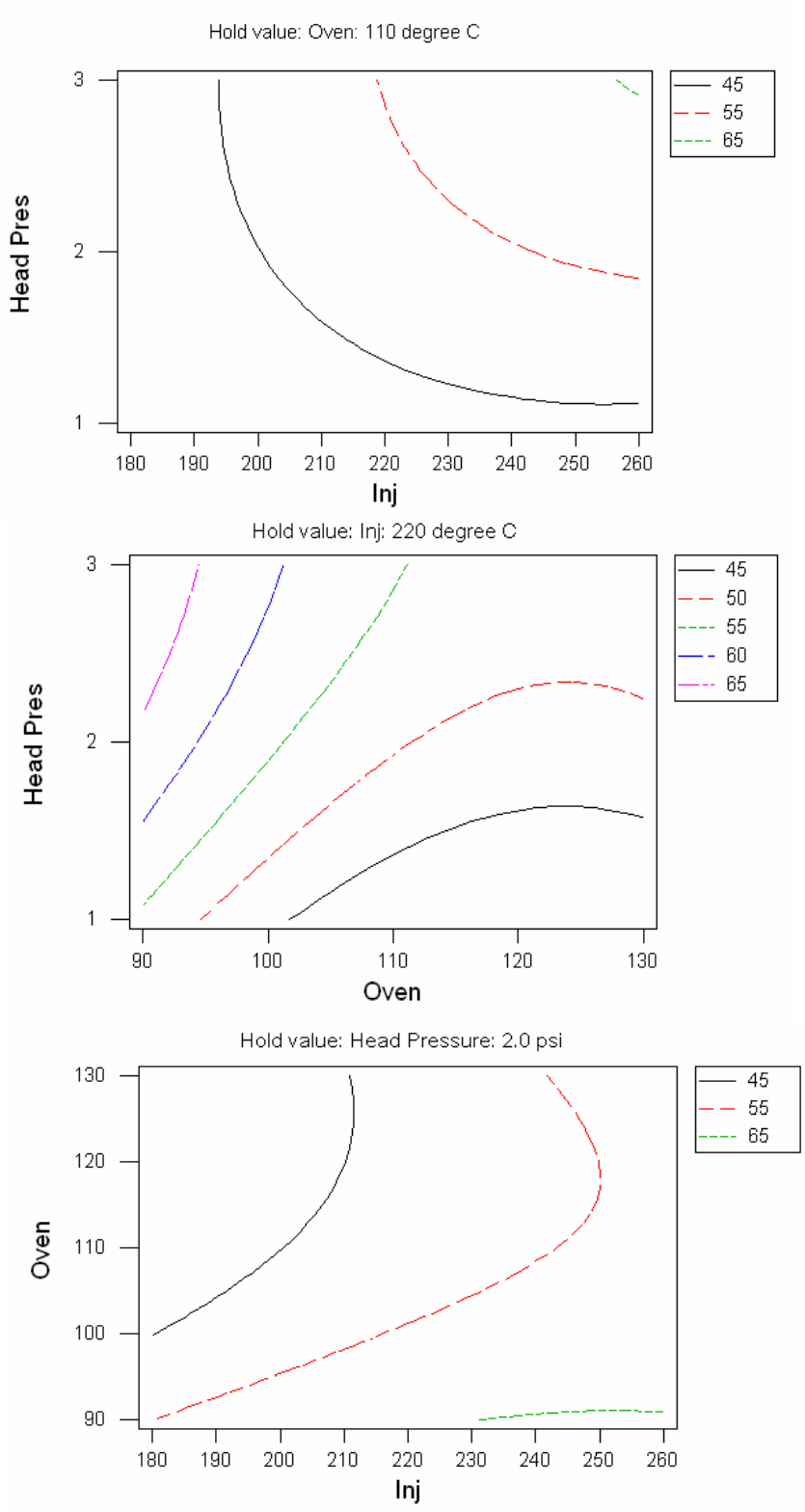

Figure 4.2 Contour plots showing the effects of injection temperature, oven temperature and head pressure for DB-5 column.

experiments in order to confirm this as well as the effect of head pressure; the results are listed in Table 4.4.

It is difficult to deduce the impact of the injection temperature and the head pressure from Table 4.4. Perhaps there is an optimal head pressure, but it is probably not practical in this case because fast analysis is desired. As for the injection temperature, it must be above some threshold where the components absorbed (adsorbed) on the fiber can be easily desorbed. If the temperature is not hot enough, it usually takes too much time to desorb the components. This leads to a longer sample plug, wider peaks, and peak overlap. Evidence for this was seen from several experiments based on an inlet temperature of 160˚C; most of the peaks tailed because of the lower injection temperature. If the temperature was too hot, the fiber could be damaged. Since the manufacturer suggested that the fibers be used within a range of 200 ˚C to 260 ˚C, all of our work was done in the range of 180 ˚C to 260 ˚C.

Figure 4.3 is the optimized results based on the observed results in Table 4.3. The optimum injection temperature, oven temperature and inlet pressure were 260 ˚C, 90 ˚C, and 3 psi, respectively, which are shown as red numbers. The chromatogram is shown in Figure 4.4. Although seven components eluted within 0.5 min, the powerful de-convolution software could identify all of them regardless of the overlap. Peak 15 is fronting because of overloading of the column.

A problem was encountered in de-convolving the peaks in the chromatogram. The relative intensities of the mass spectral peaks for each component did not fit perfectly with the NIST library. This resulted in a low correlation match; for example, peak #14, isoamyl salicylate, which is hidden underneath peak #13, methyl salicylate, can be

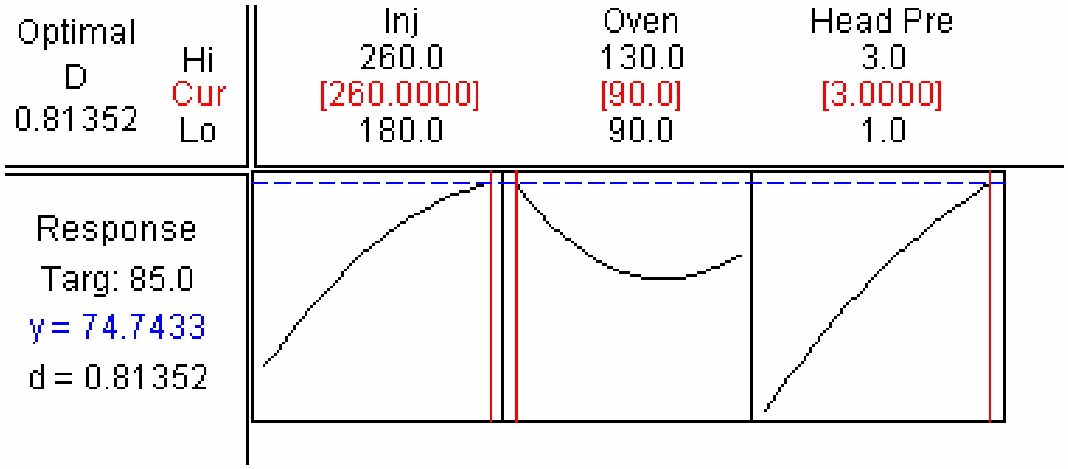

Figure 4.3 Optimized experimental conditions for DB-5 column.

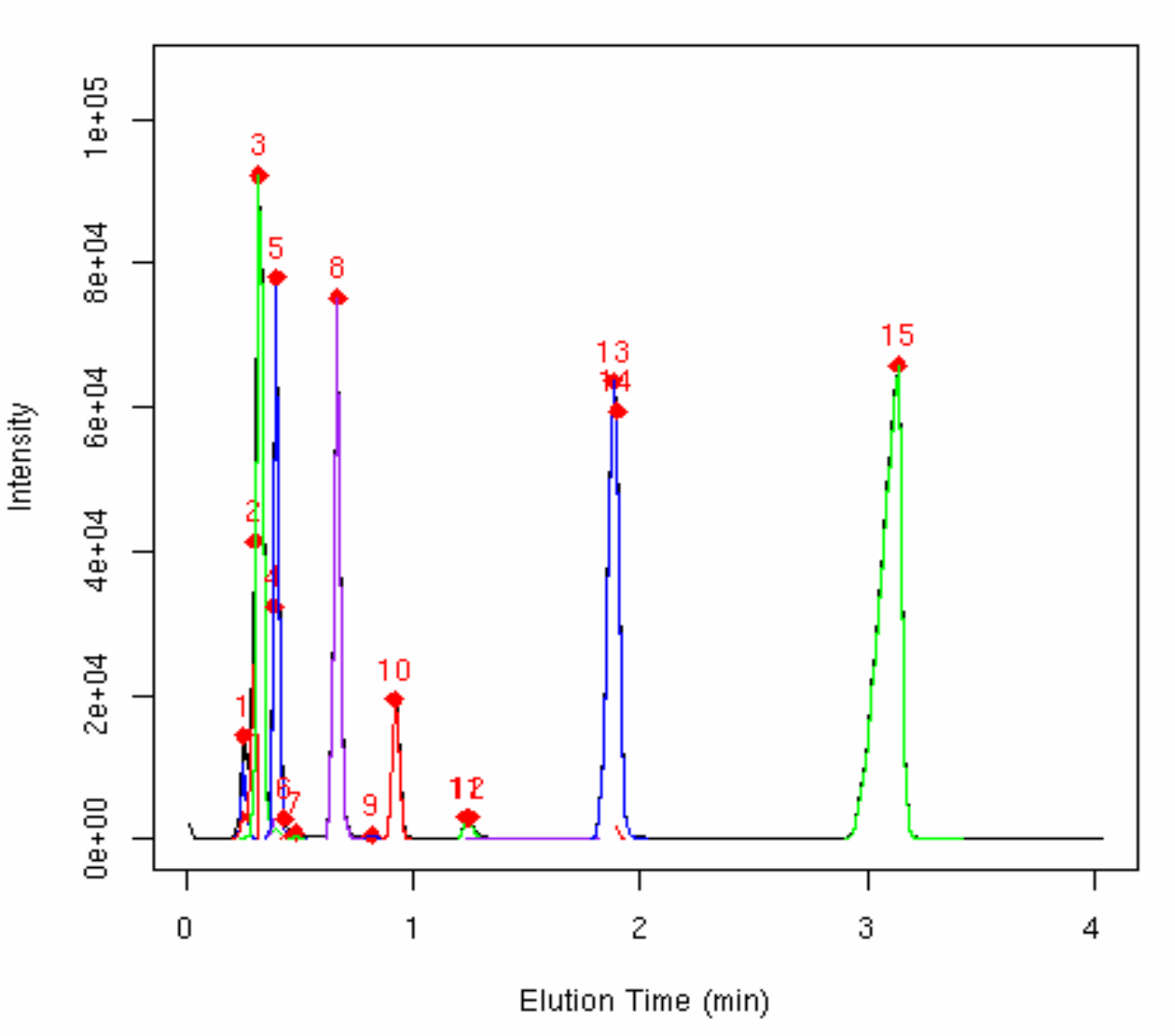

Figure 4.4 Total Ion Chromatogram obtained under the optimized conditions using a 3 m DB-5 column with 0.1 µm film thickness.

identified, however, the correlation is low (percentage match is 0.56). This is probably because the MS used was different from the one used to provide the NIST spectra, i.e., ion trap versus quadrupole or sector MS. A similar result (Table 4.5) was obtained using the 5 m DB-1701 column (0.4 μm film thickness).

The polynomial equation relating to the response with the independent variables was

$$Y=56.9133+15.030X_1+2.372X_2+6.865X_3-6.255X_1^2-3.605X_2^2-0.805X_3^2+3.708X_1X_2-0.287X_1X_3+0.477X_2X_3 \quad (4.3)$$

Once again, the equation cannot effectively reflect the real quantitative calculation of the response. Although a longer column with thicker film was used, we obtained very similar results, as can be seen in Table 4.5. In Figures 4.3 and 4.4, it can be seen that the higher the head pressure, as well as the higher the inlet temperature, the better the results. However oven temperature behaved differently. It was clear that the higher the oven temperature, the better the results. This can be explained by considering that the lower the oven temperature, the longer the analysis time. Although a good separation could be achieved, this would be traded for time according to the reciprocal of $(10+t_R)$. If the time is too long, then this will play a significant role in the evaluation.

Figure 4.8 is a chromatogram obtained under the optimized conditions. An improvement is evident in that the peak tailing for chloroacetophenone disappeared. The reason for this is due to the thicker stationary phase film and longer column used.

All in all, a 5 m DB-1701 column (0.4 μm film thickness) is the best among the columns tried with respect to higher peak capacity and resolution. However, a 3 m DB-5 column with 0.1 μm film thickness may be better when conserving power and carrier gas.

Table 4.5 Observed responses for 5 m DB-1701 column with 0.4 μm film thickness.

Run order	Injection temp (X1)	Oven temp (X2)	Head pressure (X3)	Peaks identified	Average correlation	Eyeball grade	$1/(10+t_R)$	t_R	Response (Y)
10	260	110	10	13	0.896	72	0.0391	15.6	0.455
11	260	150	10	14	0.817	80	0.0725	3.80	0.829
13	220	110	15	13	0.896	73	0.0432	13.2	0.503
14	180	130	15	14	0.874	79	0.0621	6.12	0.760
5	180	110	10	15	0.874	69	0.0389	15.7	0.510
7	220	130	10	13	0.851	78	0.0580	7.25	0.642
8	220	130	10	15	0.855	82	0.0579	7.27	0.743
14	220	150	15	14	0.827	80	0.0757	3.22	0.876
2	220	110	5	14	0.843	73	0.0337	19.7	0.398
3	220	150	5	14	0.851	79	0.0676	4.80	0.805
4	260	130	5	12	0.877	80	0.0524	9.10	0.551
15	260	130	15	15	0.876	80	0.0622	6.08	0.817
6	180	150	10	11	0.880	77	0.0723	3.83	0.700
1	180	130	5	12	0.851	76	0.0523	9.11	0.534
9	220	130	10	15	0.857	80	0.0581	7.20	0.747

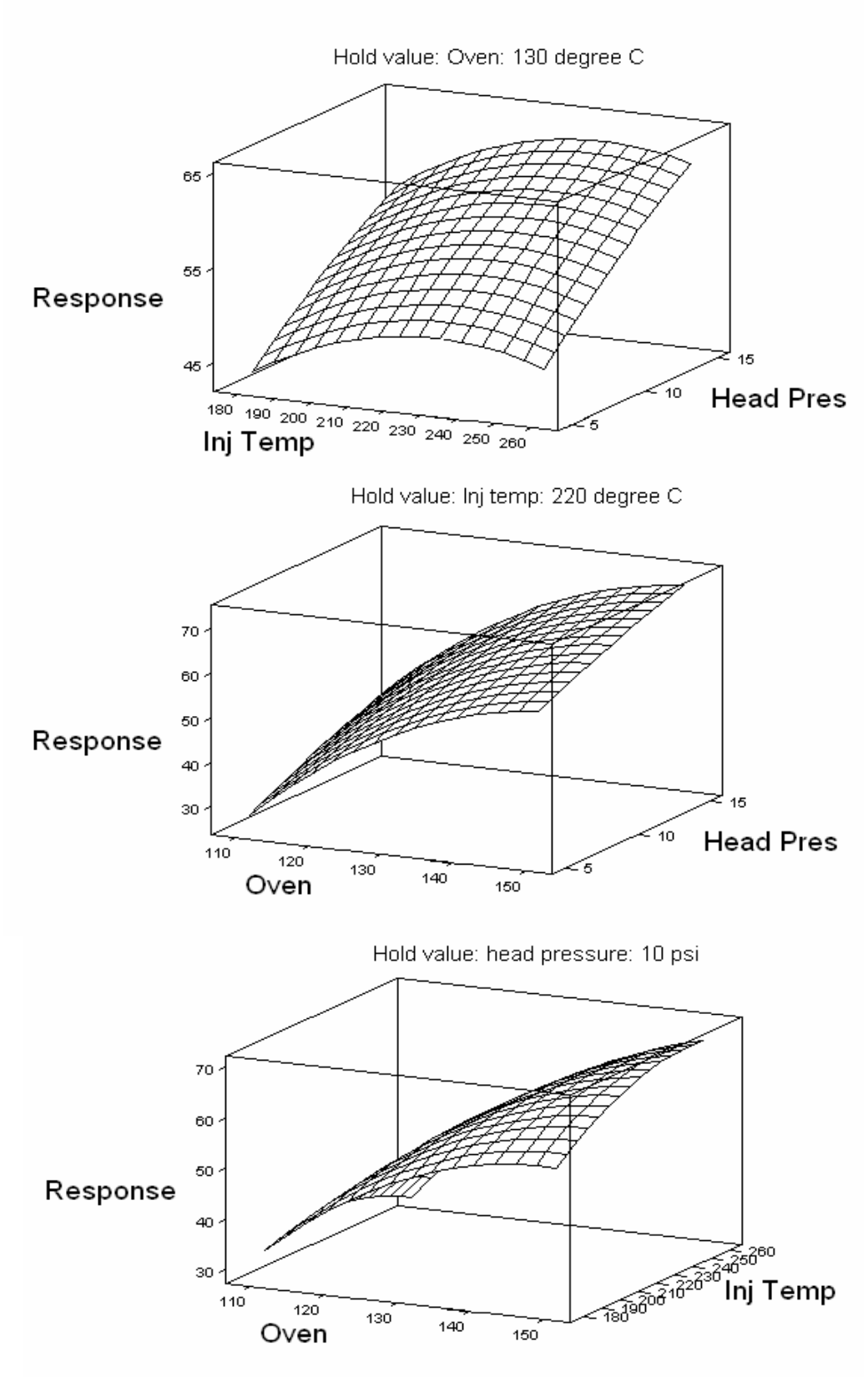

Figure 4.5 Surface response plots showing the effects of the injection temperature, oven temperature and head pressure for DB-1701 column.

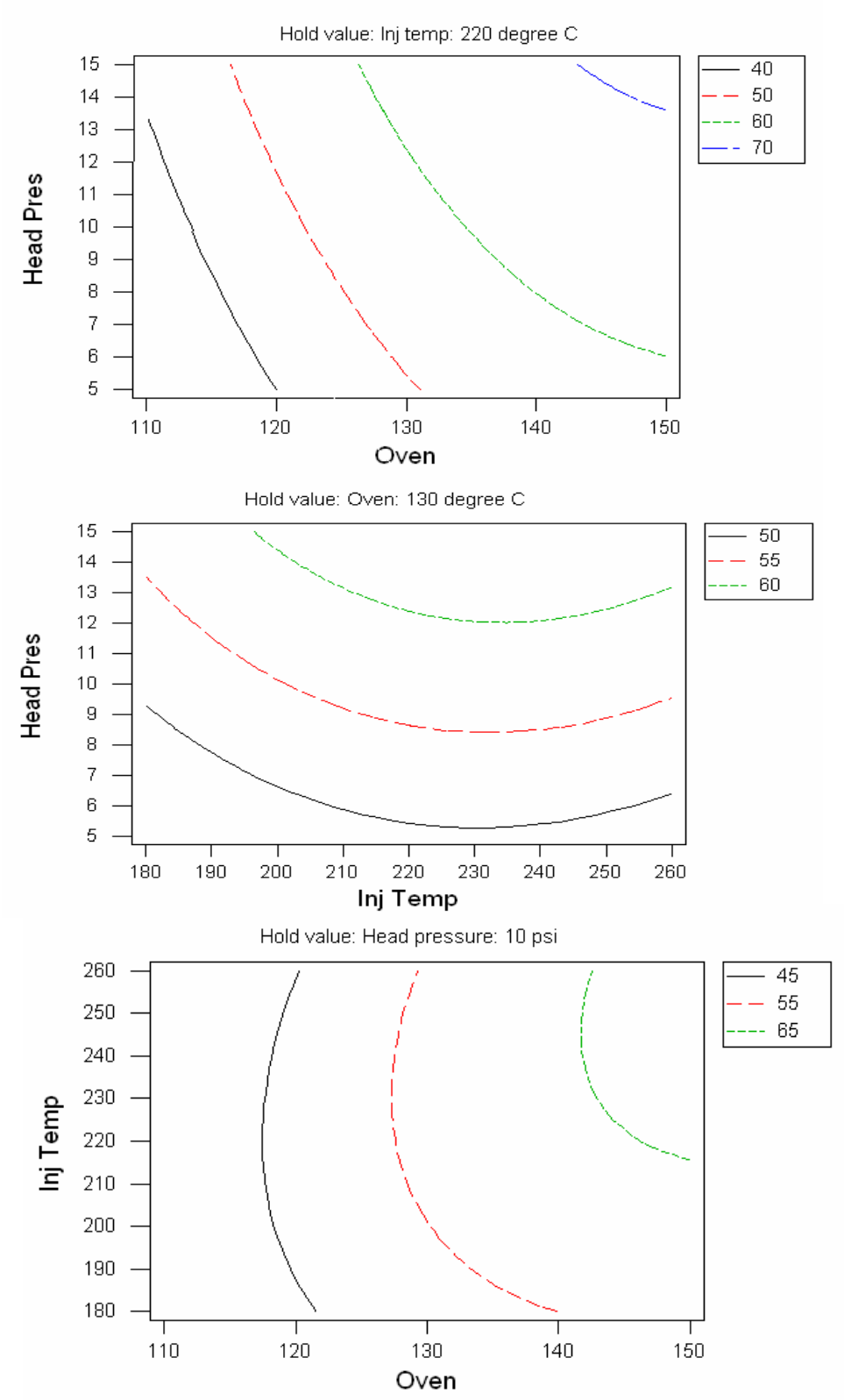

Figure 4.6 Contour plots showing the effects of the injection temperature, oven temperature and head pressure for DB-1701 column.

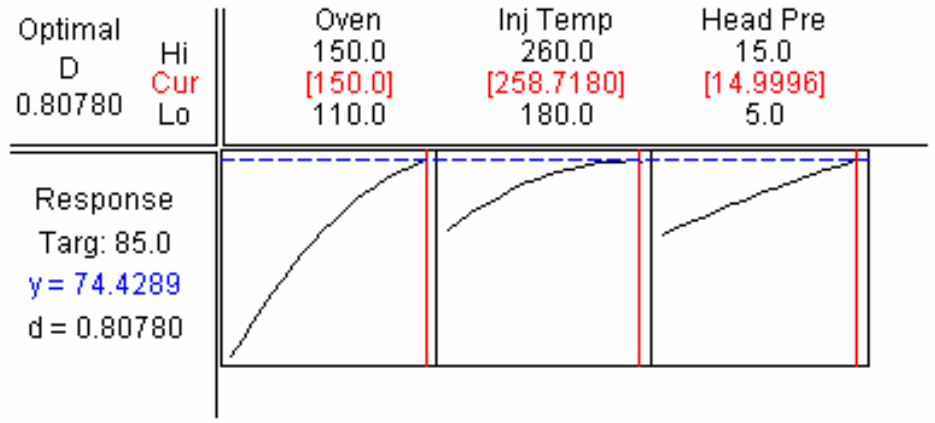

Figure 4.7 Optimized experimental conditions for DB-1701 column. Red numbers are the optimal operation conditions.

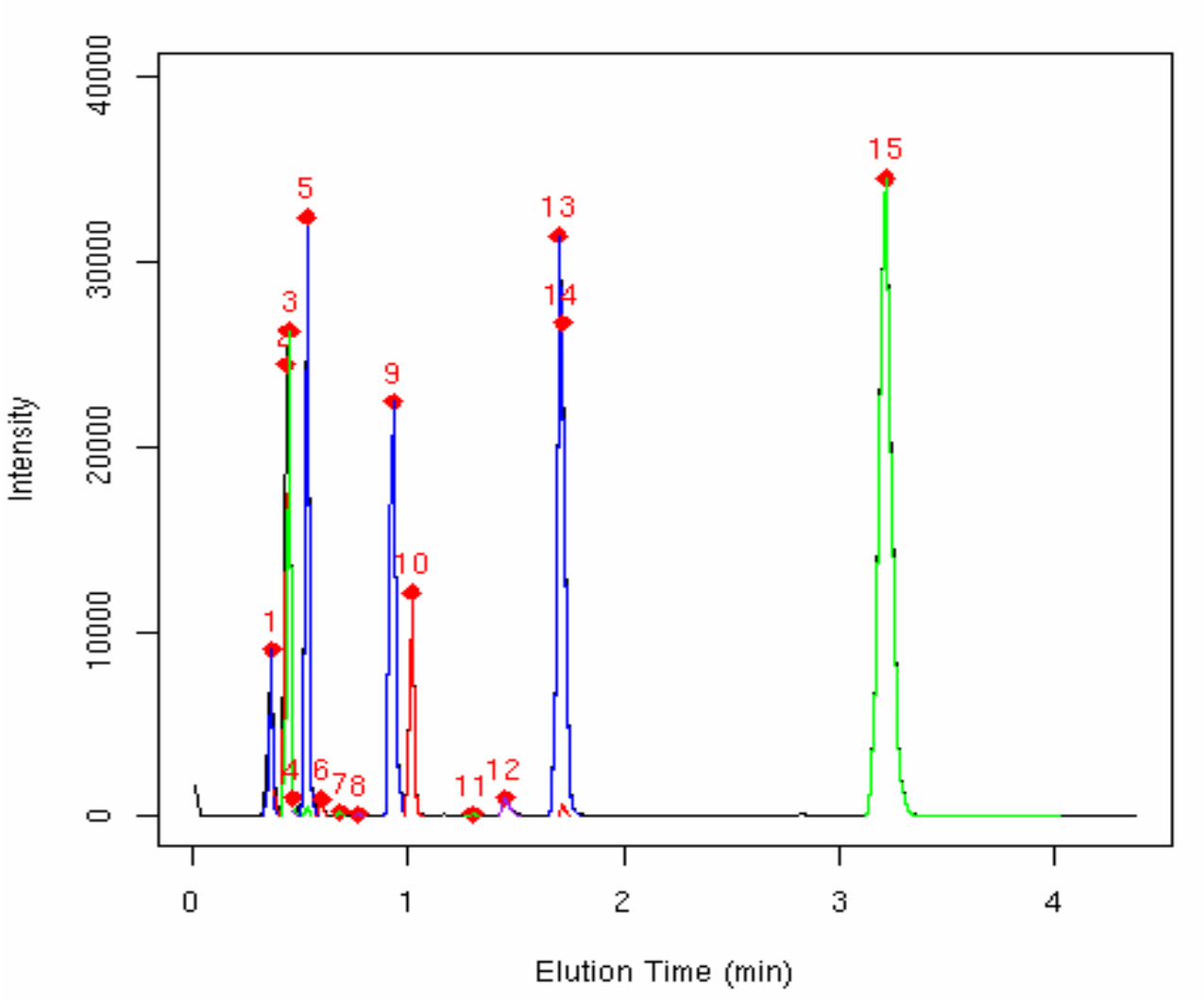

Figure 4.8 Chromatogram (TIC) obtained under the optimized conditions using a 5 m DB-1701 column with 0.4 µm film thickness.

4.5 Summary

The DB-1701 stationary phase is slightly better, but not statistically different, than the DB-5 phase. The reason for this may result from a higher correlation with the polar components identified using DB-1701, because of larger amounts of the compounds absorbed (adsorbed). However, if the amount absorbed (adsorbed) is too small, the detector response is not much higher than the background. In this case, the software will treat the analyte peaks as background resulting in a lower correlation.

The effect of the injector temperature is not significant. There is probably a threshold at which the absorbed (adsorbed) components can be desorbed within a very short time. It is necessary for this to happen because a short injection plug is needed for fast analysis.

The oven temperature behavior is slightly quadratic (concave down) with a minimum close to the high range of the experiments (200 ˚C). A lower oven temperature is probably better (it is desirable to maximize, not minimize, the Y value). There is a trade-off if time scale is considered as discussed in the results and discussion section.

Film thickness is very significant, i.e., the thicker the better. This fits theory; the thicker the film, the higher the column efficiency, and the better the resolution and peak capacity. However, a thinner stationary phase film is sometimes used to shorten the analysis time.

The head pressure is not statistically significant over the range of values of the experiments. An optimum head pressure is expected, but most likely not at the optimum flow rate.

Column length is significant and quadratic (concave down, however) with a minimum just less than 6 m. Considering the data for 3-, 5- and 10 m, it is expected that more data would show a linear relationship with longer being better. Again, when time is considered, the shorter column lengths would be preferred.

Chapter 5. Conclusions and Recommendations for Future Work

5.1 Conclusions

Separation of 24 compounds of simulants and interferents of chemical agents was studied under both temperature programming and isothermal conditions. The dependency on temperature was investigated and the theory was provided. Because of the large difference in chemical and physical properties, a good separation (i.e., good peak shape, resolution, etc.) cannot be achieved using a single column. The situation becomes much worse when performing fast separations under isothermal conditions. De-convolution software developed in the laboratory was used to identify the highly overlapped components in the chromatograms; however, the percentage correlation match with the NIST library was low for some compounds. The reason for these results may be due to limitations of the software or the differences in spectra obtained using different mass spectrometers.

All of the commercially available fibers were tested in order to find one that could absorb/adsorb most (ideally all) of the compounds. The PDMS/DVB fiber was found to be the best. SPME was successfully adapted for fast GC separation under isothermal conditions at high temperatures with short columns. The results are very promising.

Optimization of the GC conditions, such as column length, stationary phase, film thickness, column head pressure, as well as sampling procedures (i.e., sample concentration, absorption (adsorption) time, desorption time, temperature, etc.) were studied. There were no large differences seen for sampling because equilibrium of the sample between the fiber and solution can be reached quickly for the compounds tested, even at a very low concentration. There was apparently a threshold for desorption

temperature; once the temperature was above the threshold, the compounds that were absorbed (adsorbed) on the fiber could be released immediately to form a short plug, which is good for fast GC separation. If the temperature was lower than the threshold, tailing peaks were formed because of the low desorption rate.

A low polarity stationary phase should be used to separate the chemical agent compounds. The DB-5 and DB-1701 stationary phases with film thicknesses of 0.1 and 0.4 μm in 0.1 mm columns were selected for optimizing the operating conditions. Although the separation efficiency increased with increasing length and thicker stationary phase film, the analysis time also increased. This is not desirable for fast field analysis. Both 3 m DB-5 column with 0.1 μm film thickness and 5 m DB-1701 with 0.4 μm film thickness were superior to the other columns tested and gave almost the same results. Isothermal analysis at 90 ˚C or 110 ˚C under a pressure of 2 or 3 psi can be used for field analysis when time, power and carrier gas savings are considered.

5.2 Recommendations

Continuous sampling would be an advantage in field GC operation. Gradient GC is one way that enrichment of components to be separated can be achieved, and the general elution problem can be eliminated. The peak capacity using this technique should be increased based on the theory of movement of substances in a steady-state chromathermographic regime, as long as there is a steep gradient.

The use of temperature gradients was first suggested by Zhukhovisky and co-workers,[103-107] and was called chromathermography. Essentially, chromathermography is a variant of GC in which the separation occurs on the sorbent layer as a result of the

effect of the carrier gas flow in the column section where the temperature gradient is applied.

In chromathermography, the separation is additionally affected by moving the temperature gradient along the column, i.e., the column temperature varies lengthwise with time, but not simultaneously along the column as in chromatography with temperature programming.[97] Chromathermographic separation, in contrast to separation under isothermal conditions, makes it possible to increase the concentration of substances at the maximum of the chromatographic zone and, consequently, to provide greater sensitivity. The chromathermographic method is particularly effective for the separation of substances that differ greatly in their properties, e.g., boiling point. It combines the advantages of thermal desorption and elution chromatography and is applicable to the analysis of mixtures that contain components with both strong and weak sorption abilities, irrespective of their sorption isotherms.

A different operational mode for GC analyses, which is called thermal gradient programmed gas chromatography (TGPGC), involves use of time, temperature and column length from the sampling port. In TGPGC, a negative temperature gradient along the separation column is formed. Because the analytes in the carrier gas always encounter a negative temperature gradient, they become concentrated. The longer the sample stays in the column, the sharper the peak will be, and the concentration maximum in the chromatographic zone will be positioned around one characteristic temperature. When the temperature is increased, the analytes are eluted out of the column. The general elution problem encountered in conventional GC can be eliminated and a low concentration sample can be detected.

Another method of applying the thermal factor in GC is the heat dynamic method developed by Zhukhovitsky et al.[108] The heat dynamic method is a combination of frontal chromatography with a moving temperature gradient. In this method, the direction of the temperature gradient is opposite to that of the migration of the mixture to be separated. The separation is achieved in the following manner. The sample mixture is introduced into the column continuously and travels along the adsorbent layer as the temperature gradient also moves along the column. The simultaneous effects of the adsorption layer and the temperature gradient on the mixture favor its separation into individual components. According to the theory of chromatography, a given component cannot migrate along the adsorbent layer behind the point in the temperature gradient where the temperature equals the characteristic migration temperature for a given compound. It is important to note that at this point, continuous enrichment must take place (an increase in concentration). Thus, sharp peaks result.

Appendix A. Acronyms, Abbreviations, and Symbols

Acronyms and Abbreviations:

GC gas chromatography

FID flame ionization detector

TCD thermal conductivity detector

PID photoionization detector

FPD flame photometric detector

MS mass spectrometry

CIMS chemical ionization mass spectrometry

EIMS electron ionization

GC-MS gas chromatography-mass spectrometry

SAW surface acoustic wave

IMS ion mobility spectrometry

ECD electron capture detector

PFPD pulse flame photometric detector

TOF time of flight

EI electron impact or electron ionization

CIT cylindrical quadrupole ion trap

Da Dalton

MS^n tandem MS

ITMS ion trap mass spectrometry

MEMS microelectromechanical systems

RF radio frequency

MSD mass selective detector

LTM GC low thermal mass gas chromatography

TLGC transfer line gas chromatography

CE column efficiency

SPME solid phase microextraction

PDMS polydimethylsiloxane

PDMS/DVB polydimethylsiloxane/divinylbenzene

CW/DVB carbowax/divinylbenzene

DVB/CAR/PDMS divinylbenzene/carboxen/polydimethylsiloxane

PA polyacrylate

PTGC programmed temperature gas chromatography

TGPGC thermal gradient programmed gas chromatography

TIC total ion chromatogram

Symbols:

m/z mass to charge ratio

Th Dalton to charge ratio

z carbon number of paraffin

T_R **(**t_r**)** retention time

V volume

C **(**c**)** sample concentration

κ distribution or partition coefficient or the retention factor

L length of the column

v **(**u**)** velocity

K volume of stationary phase over volume of mobile phase

I retention index

ΔS molar entropy change

ΔH molar enthalpy change

α exp (ΔS /R)

β column phase ratio

r programming rate

H theoretical plate

P pressure

d_c column ID

d_f film thickness

i.d internal diameter

X spectrum of a compound with its concentration

B matrix

Y observable intensity of a certain mass

N column plate count

R resolution

Appendix B. Retention Indices for Chemical Agents, Simulants, and Interferents

ID	Chemical Warfare Agent	Retention Index	Stationary Phase
1	Ethyl N, N-dimethyl phosphoroamidocyanidate	1128.38[109]	SE-54
2	Isopropyl methyl phosphonofluoridate	791.8[110]	DB-1
3	Pinacolyl methyl phosphonofluoridate	1045.44[109]	SE-54
4	Cyclohexyl methyl phosphonofluoridate	1211.7[110]	DB-1
5	O-Ethyl-S-(2-diisopropylaminoethyl) methylphosphonothiolate	1666.7[111]	DB-1
6	Hydrogen cyanide	319.9[112]	CPSil-5 CB
7	Bis-(2-chloroethyl) sulfide	1173.59[109]	SE-54
8	Bis-(2-chloroethyl) ethylamine	1153.33[109]	SE-54
9	Bis-(2-chloroethyl) methylamine	1084.87[109]	SE-54
10	Tris-(2-chloroethyl) amine	1405.37[109]	SE-54
11	Dichloro-(2-chlorovinyl) arsine	1082.9[113]	SE-54
12	3-Quinuclidinyl benzilate	2628.4[113]	SE-54
13	Dimethyl methyl phosphonate	880.9[113]	SE-54
14	2,2-Thiodiethanol	1184.4[113]	SE-54
15	Chloroacetophenone	1290.1[113]	SE-54
16	Dibenz[b,f][1,4] oxazepine	1810.9[113]	SE-54
17	Sesquimustard	1632[114]	DB-1
18	Chlorobenzalmalononitrile	1564[113]	SE-54
19	Lewisite 2	1289.5[113]	SE-54
20	O-Ethyl-S-2-(diethylamino) ethyl methyl phosphonthiolate	1594.5[113]	SE-54
21	Isopropyl ethyl phosphonofluoridate	906.9[113]	SE-54
22	Hemisulfur mustard	1177.5[113]	SE-54
23	Bis-(2-chloroethyl) ether	984.0 [113]	SE-54
24	Triethyl phosphate	921.9[113]	SE-54
25	Trimethyl phosphate	688.8[113]	SE-54

	Interferent or Simulant		
26	Methyl salicylate	1193[115]	SE-30 or OV-1
27	Pinacolyl alcohol	634.2[113]	SE-54
28	Triethylphosphate	1109[115]	SE-30 or OV-1
29	Chlorobenzene	850.3[116]	OV-101
30	Toluene	751[117]	OV-1
31	Acetone	469.7[118]	HP-1
32	Isopropanol	483[119]	SE-30
33	Isobutyl alcohol	587[119]	SE-30
34	1-Methyl-2-pyrrolindinone	1004.9[120]	DB-1
35	Ethyl acetate	592[121]	SE-30
36	Dimethylformamide	745.9[120]	DB-1
37	2,2,4-Trimethylpentane	690[122]	Squalane
38	Diethylphthalate	1564[115]	SE-30 or OV-1
39	2-Chlorophenol	987[123]	SE-30
40	Parathion	1942[124]	SE-30 or OV-1
41	Ethanol	446[119]	SE-30
42	Ethylene glycol	798[125]	SE-30
43	Dimethyl sulfoxide	781.9[114]	DB-1
44	Isoamyl salicylate	1515.4[126]	SE-30
45	2-Methyl-2,4-pentanediol	963[125]	SE-30
46	4-Hydroxy-4-methyl-2-pentanone	830[124]	SE-30 or OV-1
47	Acetic acid	642[119]	SE-30
48	Ascorbic acid	2120[127]	SE-30 or OV-1
49	Diethyl malonate	1038.2[114]	DB-1
50	Tributyl phosphate	1615.6[114]	DB-1

Appendix C. Mass Spectral Data [128]

ID	Chemical Warfare Agent	Ion m/z Abundance					
		1	2	3	4	5	Highest m/z
1	Ethyl N, N-dimethyl phosphoroamidocyanidate	43	70	44	133	162	163
		999	850	550	420	290	10
2	Isopropyl methyl phosphonofluoridate	99	125	81	43	41	126
		999	330	100	80	70	10
3	Pinacolyl methyl phosphonofluoridate	126	99	82	69	41	127
		999	850	500	490	370	40
4	Cyclohexyl methyl phosphonofluoridate	99	67	54	41	39	137
		999	200	140	80	60	20
5	O-Ethyl-S-(2-diisopropylaminoethyl) methylphosphonothiolate	114	72	127	70	30	252
		999	210	130	90	80	20
6	Hydrogen cyanide	27	26	12	13	14	29
		999	168	42	17	17	1
7	Bis-(2-chloroethyl) sulfide	109	63	111	27	45	162
		999	480	360	280	210	1
8	Bis-(2-chloroethyl) ethylamine	120	65	122	92	57	171
		999	400	330	180	140	20
9	Bis-(2-chloroethyl) methylamine	106	108	63	44	42	159
		999	15	229	214	166	4
10	Tris-(2-chloroethyl) amine	154	156	63	56	27	203
		999	640	540	360	220	10
11	Dichloro-(2-chlorovinyl) arsine	145	110	206	208	147	212
		999	800	760	740	670	10
12	3-Quinuclidinyl benzilate	183	105	126	77	111	338
		999	540	530	340	340	20
13	Dimethyl methyl phosphonate	94	79	109	93	124	124
		999	770	410	330	210	210
14	2,2-Thiodiethanol	61	45	31	104	91	124
		999	683	383	357	337	2
15	Chloroacetophenone	105	77	51	106	50	156
		999	521	157	77	56	3
16	Dibenz[b,f][1,4] oxazepine	195	167	166	139	51	197
		999	725	379	343	229	12

17	Sesquimustard	123	63	45	109	73	223
		999	766	676	659	554	1
18	Chlorobenzalmalononitrile	153	188	50	75	51	191
		999	596	342	342	307	28
19	Lewisite 2	87	51	89	145	147	235
		999	402	346	339	241	5
20	O-Ethyl-S-2-(diethylamino) ethyl methyl phosphonthiolate	86	99	58	79	84	238
		999	220	70	70	60	1
21	Isopropyl ethyl phosphonofluoridate	113	139	43	84	41	163
		999	350	80	60	60	2
22	Hemisulfur mustard	61	110	45	47	35	114
		999	260	216	211	127	4
23	Bis-(2-chloroethyl) ether	93	63	27	95	65	144
		999	641	365	320	206	7
24	Triethyl phosphate	82	65	83	111	81	167
		999	850	608	507	498	12
25	Trimethyl phosphate	93	109	63	124	94	126
		999	572	465	393	279	2
	Stimulant or Interferent						
26	Methyl salicylate	120	92	152	39	121	153
		999	577	412	353	323	37
27	Pinacolyl alcohol	57	45	56	41	87	103
		999	750	625	387	287	5
28	Triethylphosphate	99	155	127	81	109	183
		999	736	536	503	354	3
29	Chlorobenzene	112	77	114	51	50	116
		999	453	329	120	96	1
30	Toluene	91	62	65	39	63	94
		999	621	85	73	45	1
31	Acetone	43	58	15	27	42	60
		999	331	305	75	68	1
32	Isopropanol	45	43	27	41	29	61
		999	142	93	62	53	1
33	Isobutyl alcohol	43	31	42	41	33	75
		999	668	569	555	507	4
34	1-Methyl-2-pyrrolindinone	99	44	98	42	41	100
		999	889	796	597	376	66

35	Ethyl acetate	43	29	45	61	27	89
		999	208	138	123	122	2
36	Dimethylformamide	73	44	42	30	28	74
		999	860	360	220	200	40
37	2,2,4-Trimethylpentane	57	41	56	43	29	100
		999	309	283	238	158	1
38	Diethylphthalate	149	177	150	65	29	223
		999	273	125	84	81	5
39	2-Chlorophenol	128	64	130	63	65	131
		999	520	320	260	180	20
40	Parathion	291	109	97	139	137	294
		999	714	704	419	406	6
41	Ethanol	31	45	29	27	46	47
		999	514	298	224	216	7
42	Ethylene glycol	31	33	29	32	43	62
		999	353	126	106	63	26
43	Dimethyl sulfoxide	63	78	45	61	15	80
		999	761	324	169	117	25
44	Isoamyl salicylate	120	43	121	138	39	209
		999	485	366	361	290	20
45	2-Methyl-2,4-pentanediol	59	43	41	56	45	104
		999	391	286	254	227	3
46	4-Hydroxy-4-methyl-2-pentanone	43	59	58	101	42	102
		999	248	201	98	57	6
47	Acetic acid	43	45	60	15	42	62
		999	938	636	345	202	2
48	Ascorbic acid	116	43	85	61	29	178
		999	282	180	178	149	1
49	Diethyl malonate	29	115	43	133	88	161
		999	532	526	289	198	2
50	Tributyl phosphate	99	155	41	29	57	267
		999	261	157	127	106	2

References

1. Convention on the Prohibition of the Development, Production, Stockpiling and Use of Chemical Weapons and on their Destruction, Technical Secretariat of the Organization for Prohibition of Chemical Weapons, The Hague, **1997.**
2. Mesilaakso, M.; Ratio. M. *Encyclopedia of analytical chemistry*; Wiley: New York, **2000**; PP. 899.
3. O. Kostiainen, Forensic Science, In: *Handbook of Analytical Separations*, vol. 2, M. J. Bogusz (Ed.), Elsevier Science: Amsterdam, **2000**, PP. 405.
4. Hooijschuur, E. W. J.; Kientz, C. E.; Brinkman, U. A. *J. Chromatogr. A* **2002**, 982, 177.
5. Witkiewicz, Z.; Mazurek, M.; Szulc. J. *J. Chromatogr*. **1990,** 503, 293.
6. Rautio, M., Ed., *Recommended Operating Procedures for Sampling and Analysis in the Verification of Chemical Disarmament*: **1993**.
7. Reddy, T. J.; Vijaya Saradhi, U. V. R.; Prabhakar, S.; Vairamani, M. *J. Chromatogr. A* **2004,** 1038, 225.
8. Henry, C. *Anal. Chem*. News Features, **1997**, March, p 195.
9. McClennen, W. H.; Arnold, N. S.; Meuzelaar, H. L. C. *Trends in Anal. Chem*. **1994,** 13(7), 286.
10. Lammert, S. A. *12th Sanibel conference on field-portable and miniature mass spectrometry*, **2000,** Sanibel Island, FL, USA.
11. Diaz, J. A.; Daley, P.; Miles, R.; Rohrs, H.; Polla, D. *Trends in Anal. Chem.* **2004**, 23, 314.
12. Diaz, J. A.; Giese, C. F.; Gentry, W. R. *J. Am. Soc. Mass Spectrom*. **2001**, 12, 619.
13. Diaz, J. A.; Giese, C. F.; Gentry, W. R. *Field Anal. Chem. Technol*. **2001**, 5,157.
14. Andresen, B. D.; Eckels, J. D.; Kinnons, J. F.; Myers, D. W. patent 5525799, **1996.**
15. Shortt, B. J.; Darrach, M. R.; Holland, P. M.; Chutjian, A. *J. Mass Spectrom.* **2005**, 40, 36.
16. Holland, P. M.; Chutjian, A.; Darrach, M. R.; Orient, O. J. *Proc. SPIE* **2003**: 4878:1
17. Orient, O. J.; Chutjian, A. *Rev. Sci. Instrum*. **2002**, 73, 215.
18. Orient, O. J.; Chutjian, A. *Rev. Sci. Instrum*. **2003**, 74, 2936.

19. Urban, D. T. Arnold, N. S.; Meuzelaar, H. L. C. *Proceedings of the 28 ASMS conference on mass spectrometry and applied topics;* **1990,** p 615.
20. Haas, J. S. Bushman, J. F.; Howard, D. E.; Wong, J. L.; Eckels, J. D. patent 6351983 B1, March. 5, **2002.**
21. FemtoScan, Midvale, UT. NSF, SBIR Phase1; **1998.**
22. Smith, P. A.; Lepage, C. R. J.; Koch, D.; Wyatt, H. D. M.; Hook, G. L.; Betsinger, G.; Erickson, R. P.; Eckenrode, B. A. *Trends in Anal. Chem.* **2004**, 23, 296.
23. Hail, M. E.; Yost, R. A. *Anal. Chem*. **1989,** 61, 2410.
24. Rubey, W. A. US Patent 5028243, **1991**.
25. Ehrmann, E. U.; Dharmasena, H. P.; Carney, K.; Overton, E. B. *J. Chromatogr. Sci.* **1996**; 34: 533.
26. Overton, E. B.; Carney, K. R. US Patent 5 611 846, **1997**.
27. Sloan, K. M.; Mustacich, R. V.; Eckenrode B. A. *Field Anal. Chem. Technol*. **2001**, 5, 288.
28. Smith, P. A.; Sng, M. T.; Eckenrode, B. A.; Leow, S. Y.; Koch, D.; Erickson, R. P.; Lepage, C. R. J.; Hook, G. L. *J. Chromatogr. A* **2005**, 1067, 285.
29. http://www.diab.com/appnotes/tlgcms2.htm
30. Doherty, S. J.; Winniford, W. L.; Hein, S. J. *42nd ASMS Conference on Mass Spectrometry,* **1994**, Chicago, IL, USA.
31. Doherty, S. J. *42nd ASMS Conference on Mass Spectrometry*, **1994**.
32. Mcclennen, W. H.; Vaughn, C. L.; Cole, P. A.; Sheya, S. N.; Wager, D. J.; Mott, T. J.; Dworzanski, J. P.; Arnold, N. S.; Meuzelaar, H. L. C. *Field Anal. Chem.* Technol. **1997**, 1, 109.
33. Arnold, N. S.; Dworzanski, J. P.; Sheya, S. A.; McClennen, W. H.; Meuzelaar, H. L. C. *Field Anal. Chem. Technol*. **2000**, 4, 219.
34. Snow, N. H. *J. Liq. Chromatogr.* **2004**, 27, 1317.
35. Song, X.; McNair, H. *J. Chromatogr. Sci*. **2002**, 40, 321.
36. Van Deursen, M.; Beens, J.; Cramers, C.; Janssen, H. G. *J. High Resol. Chromatogr*. **1999**, 22, 509.
37. Dalluge, J.; Ou-Aissa, R.; Vreuls, J. J.; Brinkman, U. A. Th. *J. High Resol. Chromatogr.* **1999**, 22, 459.

38. Jennings, W. J. *Analytical Gas Chromatography*; Academic Press: Orlando, FL, **1987**; PP.77.
39. Terry, S. C.; Jerman, J. H.; Angell, J. B. *IEEE Trans*. ED., **1979,** PP. 1880.
40. http://www.eecs.umich.edu/~jpotkay/MEMS03_365_Potkay.pdf
41. Personal correspondence with Dr. Sacks.
42. Lee, M. L.; Vassilaros, D. L.; White, C. M.; Novotny, M. *Anal. Chem*. **1979**, 51, 768.
43. Gohlke, C. *Anal. Chem.* **1959,** 31, 535.
44. http://www.has.vcu.edu/che/people/bio/fenn.html
45. Skoog, D. A.; Holler, F. J.; Nieman, T. A. *Principles of Instrumental Analysis*, fifth edition, Harcourt Brace & company, Orlando, Florida. **1998**.
46. Personal correspondence with Simon Zipper Lomas from Phenomenex, Inc.
47. Zhang, Z.; Yang, M. J.; Pawliszyn J. *Anal. Chem*. **1994**, *66*, 844A.
48. Scheppers Wercinski, A. S. *Solid Phase Microextraction: a practical guide*; Marcel Dekker: New York, **1999**.
49. Pawliszyn, J. *Applications of Solid Phase Microextraction*; Cambridge: Royal Society of Chemistry, **1999**.
50. D'Agostino, P. A.; Provost, L. R.; Anacleto J. F.; Brooks, P. W. *J. Chromatogr.* **1990,** 504, 259.
51. Batlle, R.; Sánchez, C.; Nerin, C. S. *Anal. Chem*. **1999**, 71, 2417.
52. Bagheri H.; Mohammadi, A. *J. Chromatogr. A* **2003,** 1011, 1.
53. Mester, Z.; Sturgeon, R.; Pawliszyn, J. *Spectrochim. Acta B* **2001**, 56, 233.
54. Sides, S. L.; Polowy, K. B.; Thornquest, A. D.; Burinsky, D. J. *J. Pharm. Biomed. Anal.* **2001**, 25, 379.
55. Karaisz, K. G.; Snow, N. H. *J. Microcol. Sep*. **2001**, 13, 1.
56. Coran, S. A.; Giannellini, V.; Furlanetto, S.; Bambagiotti-Alberti, M.; Pinzauti, S. *J. Chromatogr. A* **2001**, 915, 209.
57. Frost, R. P.; Hussain, M. S.; Raghani, A. R. *J. Sep. Sci*. **2003,** 26, 1097.
58. Theodoridis, G.; Koster, E. H. M.; de-Jong, G. J. *J. Chromatogr. B* **2000**, 745, 49.
59. Snow, N. H. *J. Chromatogr. A* **2000**, 885, 445.
60. Ulrich, S. *J. Chromatogr. A* **2000**, 902, 167.
61. Kataoka, H.; Lord, H. L.; Pawliszyn, J. *J. Chromatogr. A* **2000**, 880, 35.

62. Lakso, H. A.; Ng, W. F. *Anal. Chem*. **1997**, 69, 1866.
63. Alcaraz, A.; Hulsey, S. S.; Whipple, R. E.; Andersen in Heyl, M. and McGuire; R. (Eds.), *analytical chemistry associated with the destruction of chemical weapon;* Kluwer Academic Publishers: Netherlands **1997**, PP 65.
64. Sng, M. T.; Ng, W. F. *J. Chromatogr. A* **1999**, 832, 173.
65. Schneider, J. F.; Boparai, A. S.; Reed, L. L. *J. Chromatographic. Sci*. **2001**, 39, 420.
66. Hook, G. L.; Lepage, C. J.; Miller, S. I.; Smith, P. A. *J. Sep. Sci*. **2004**, 27, 1017.
67. Smith, P. A.; Sheely, M. V.; Kluchinsky, T. A. Jr. *J. Sep. Sci*. **2002**, 25, 917.
68. Kimm, G. L.; Hook, G. L.; Smith, P. A. *J. Chromatogr. A* **2002**, 971, 185.
69. Hook, G. L.; Kimm, G.; Betsinger G.; Savage, P. B.; Swift, A.; Logan, T.; Smith, P. A. *J. Sep. Sci*. **2003**, 26, 1091.
70. Louch, D.; Mothlagh, S.; Pawliszyn, J. *Anal. Chem*. **1992**, *64*, 1187.
71. Zhang, Z.; Pawliszyn, J. *Anal. Chem*. **1993**, *65*, 1843.
72. Brereton, R. G. *Chemometrics: Application of Mathematics and Statistics to Laboratory Systems*, Ellis Horwood, Chichester, **1990**.
73. Davies, L. *Efficiency in Research, Development and Production: The Statistical Design and Analysis of Chemical Experiments*, Royal Society of Chemistry, **1993**.
74. Górecki T.; Pawliszyn J. *J. High Resol. Chromatogr*. **1995**, 18, 161.
75. Griffiths, J. H.; James, D. H.; Phillips, O. S. *Analyst* (London) **1952,** 77, 897.
76. Harris, W. E.; Habgood, H. W. *Programmed Temperature Gas Chromatography*; Wiley: New York, London, Sydney, 1966.
77. Golay W. J. E. "theory of chromatography in open and coated tubular columns with round and rectangular cross-sections" in *Gas Chromatography* **1985**, Royal Tropical Institute, Amsterdam, May 19-23, **1958**. Desty, D. H. Ed. Academic Press. New York, NY, **1958**
78. Klee, M. S.; Blumberg, L. M. *J. Chromatogr. Sci*. **2002**, 40, 234.
79. Desty, D. H.; Goldup, A.; Swanton, W. T. "performance of coated capillary columns". In *Gas Chromatography,* Kellogg Center for Continuing Education, Michigan State University, June 13-16, **1961**. N. Brenner, J. E. Callen, and M. D. Weiss, Ed. Academic Press: New York, NY, **1962**, PP 105.

80. Guiochon, G.; Guillemin, C. L. *Quantitative gas chromatography*; Elsevier: Amsterdam, **1988**.
81. Stolyarov, B. V.; Savinov, I. M.; Vitenberg, A. G.; Kartseva, L. A.; Zenkevich, L. G.; Kalmanovskaya, V. I.; Kalambet, Y. A, *Prakticheskaya gazovaya I zhidkostnaya kromatografiya (practical gas and liquid chromatography*); Izd St. Petersburg, Universiteta, St. Petersburg, **1998**.
82. A. Van Es, *High-speed narrow bore capillary gas chromatography*; Hüthig, Heidelberg, **1992**.
83. Verezkin; V. G.; Lapin, A. B.; Malyukova, I. V. *J. Chromatogr. A* **2001,** 919, 357.
84. Cramers, C. A.; Scherpenzeel, G. J.; Leclercq, P. A. *J. Chromatogr*. **1981,** 203, 207.
85. Cramers, C. A. and Leclercq, P. A. *CRC Critical Reviews in Analytical Chemistry*; CRC Press, Inc.: Boca Raton, FL, **1988**, Vol. 20, Chapter 2, p 117.
86. Schutjes, C. P. M.; Vermeer, E. A.; Rijks, J. A.; Cramers, C. A. *J. Chromatogr*. **1982,** 253, 1.
87. Cramers C. A.; Leclercq, P. A. *J. Chromatogr. A* **1999,** 842, 3.
88. Kováts, E. *Helv Chim Acta* VII: 1915-1932, **1958**.
89. van Den Dool, H.; Kratz, P. Dec. *J. Chromatogr*. **1963,** 11, 463.
90. Messadi, D.; Ali-Mokhnache, S. *Chromatographia* **1993,** 37, 264.
91. Vezzani, S.; Moretti, P.; Castello, G. *J. Chromatogr. A* **1994,** 677, 331.
92. Akporhonor, E. E.; Le Vent, S.; Taylor D. R. *J. Chromatogr*. **1990,**504, 269.
93. Snijders, H.; Janssen, H.; Cramers, C. *J. Chromatogr. A* **1995,** 718, 339.
94. Curvers, J.; Rijks, J.; Cramers, C. *J. High Resol. Chromatogr. Chromatogr. Commun*. **1985**, 8, 607.
95. Guan, Y.; Li, L.; Zhou, L. *J. High. Resol. Chromatogr*. **1995,** 18, 593.
96. Guan, y.; Zhou, L. *J. Chromatogr*. **1991,** 552, 187.
97. Zhukhovitsky, A. A.; Trukel'taub, N. M. *Gazovaiya Khromatografiya* (gas chromatography), Gostoptekhizdat, Moscow, **1962**.
98. Jennings, W. *International Symposium for Capillary Electrophoresis and Chromatography.* May 22-25, **2005**, Las Vegas, Nevada.
99. Personal correspondence with Jim Wheeler from Agilent Technologies

100. Schmidt, S. R.; Launsby, R. G. *Understanding Industrial Designs Experiments*. Air Academy Press, Colorado Springs, Colorado, **1998**, PP 1.
101. Box, G. E. P.; Behnken, D. W. *Technometrics* **1960**, 2 (4), 455.
102. Oliphant, J. R.; Tolley, H. D.; Rockwood, A. L.; Lee, E. D.; Lee, M. L. U.S. Patent 0258357 A1, **2005**.
103. Zhukhovitsky, A. A.; Trukel'taub, N. M.; Sokolov, V. A. Dokl.Akad. Nauk SSSR **1953**, 88, 859.
104. Trukel'taub, N. M.; Shvartsman, V. P.; Georievskaya, T. V. Zh. Fiz.Khim. **1953**, 27, 1827.
105. Zhukhovitsky, A. A.; Trukel'taub, N. M. Dokl.Akad. Nauk SSSR **1954**, 94, 77.
106. Zhukhovitsky, A. A.; Trukel'taub, N. M.; Shvartsman, V. P. Zh, Fiz. Khim. **1954**, 28, 1901.
107. Zhukhovitsky, A. A.; Trukel'taub, N. M. Solotareva, O. V.; Sokolov, V. A. Dokl. Akad. Nauk SSSr, **1951,** 77, 435.
108. Zhukhovitsky, A. A.; Trukel'taub, N. M.; Georgievskaya, T. B. Dokl.Akad. Nauk SSSR **1953**, 92, 987.
109. Kaipainen, A.; Kostiainen, O.; Riekkola, M-L. *J. Microcol. Sep*. **1992**, 4, 245.
110. D'Agostino, P. A.; Provost, L. R. *J. Chromatogr*. **1985**, 331, 47.
111. D'Agostino, P. A.; Provost,L. R.; Visentini, J. *J. Chromatogr*. **1987**, 402, 221.
112. Do, L.; Raulin, F. *J. Chromatogr*. **1992**, 591, 297.
113. Encyclopedia of Analytical Chemistry, Instrumentation and Applications Section, R.A. Meyers, Wiley, **2000**, PP 963.
114. Hancock, J. R. *J. Chromatogr***. 1991**, 538, 249.
115. Ardrey, R. E.; Moffat, A. C. *J. Chromatogr*. **1981**, 220, 195.
116. Hassani, A.; Meklati, B. Y. *Chromatographia* **1992**, 33, 267.
117. Guan, Y.; Kiraly, J.; Rijks, J. A. *J. Chromatogr*. **1989**, 472, 129.
118. Heberger, K.; Gorgenyi, M. *J. Chromatogr. A* **1999**, 845, 21.
119. Peng, C. T.; Ding, S. F.; Hua, R. L.; Yang, Z. C. *J. Chromatogr*. **1988**, 436, 137.
120. Calculated according to Agilent Technologies catalog.
121. Ashes, J. R.; Haken, J. K. *J. Chromatogr*. **1974**, 101, 103.

122. Budahegyi, M. V.; Lombosi, E. R.; Lombosi, T. S.; Meszaros, S. Y.; Nyiredy, Sz.; Tarjan, G.; Timar, I.; Takacs, J. M. *J. Chromatogr*. **1983**, 271, 213.
123. Korhonen, I. O. O. *J. Chromatogr*. **1984**, 315, 185.
124. Indices of Toxicologically Relevant Substances on SE-30 or OV-1, 1985, VCH publisher, 3rd ed., 1985.
125. McReynolds W. O. *Gas Chromatographic Retention data*, **1966**, PP 299.
126. Tudor, E. *J. Chromatogr. A*. **1997**, 779, 287.
127. De Zeeuw, R. A.; Franke, J. P. Maurer, H. H.; Pfleger, K. 3rd ed. *Gas Chromatographic Retention Indices of Toxicologically Relevant Substances on SE-30 or OV-1*, **1992**.
128. Data from the NIST/EPA/NIH Mass Spectral Library (1998). The data are simplified for presentation, and include the five most abundant peaks and the highest m/z ration ion observed. Each entry includes both m/z ration (upper number) and relative abundance (lower number, based on a maximum of 1000) for each ion.